Efficient Synthesis of Mannopyranoside-Based Fatty Acyl Esters: Effects of Acyl Groups on Antimicrobial Activities

Md. Lutfor Rahaman , Md. Atiqur Rahman , Md. Mohin Hasnain , Mohammad Amran , Talha Bin Emran , Md Ashikur Rahaman Khan , Md. Abdul Majed Patwary , Mohsin Kazi * , Mohammed Mahbubul Matin *

Posted Date: 6 November 2023

doi: 10.20944/preprints202311.0365.v1

Keywords: ADMET; antimicrobial agents; effects of chain length; molecular docking; regioselective acylation; structure-activity relationship; sugar fatty acid ester (SFAE).

Article

Efficient Synthesis of Mannopyranoside-Based Fatty Acyl Esters: Effects of Acyl Groups on Antimicrobial Activities

Md. Lutfor Rahaman [1], Md. Atiqur Rahman [1], Md. Mohin Hasnain [1], Mohammad Amran [1], Talha Bin Emran [2,3], Md Ashikur Rahaman Khan [1], Md. Abdul Majed Patwary [4], Mohsin Kazi [5,*] and Mohammed Mahbubul Matin [1,*]

[1] Bioorganic and Medicinal Chemistry Laboratory, Department of Chemistry, Faculty of Science, University of Chittagong, Chittagong, 4331, Bangladesh; mdlutforrahamanchem@gmail.com (M.L.R.); atiqchemcu@gmail.com (M.A.R.); mohinhasnain132@gmail.com (M.M.H.); alamranchemcu@gmail.com (M.A.); ashikurk@gmail.com (M.A.R.K.); mahbubchem@cu.ac.bd (M.M.M.)
[2] Department of Pathology and Laboratory Medicine, Warren Alpert Medical School & Legorreta Cancer Center, Brown University, Providence, RI 02912, USA; talha_bin_emran@brown.edu (T.B.E.)
[3] Department of Pharmacy, BGC Trust University Bangladesh, Chittagong 4381, Bangladesh; talhabmb@bgctub.ac.bd (T.B.E.)
[4] Department of Chemistry, Comilla University, Cumilla, 3506, Bangladesh; mamajedp@gmail.com (M.A.M.P.)
[5] Department of Pharmaceutics, College of Pharmacy, PO BOX 2457, King Saud University, Riyadh, 11451, Saudi Arabia; mkazi@ksu.edu.sa (M.K.)
* Correspondence: mahbubchem@cu.ac.bd; Tel.: +880 1716 839689 (M.M.M.); mkazi@ksu.edu.sa (M.K.)

Featured Application: The fatty acid chain length of mannopyranoside (MDM) esters significantly affects their antifungal activity. An efficient method for selective acylation of MDM is described, where esters with the C8 chain substituted at the 6-*O* position were more active in the fungal inhibition. Also, mannopyranoside oligoesters may be suitable to develop pharmaceutically useful materials.

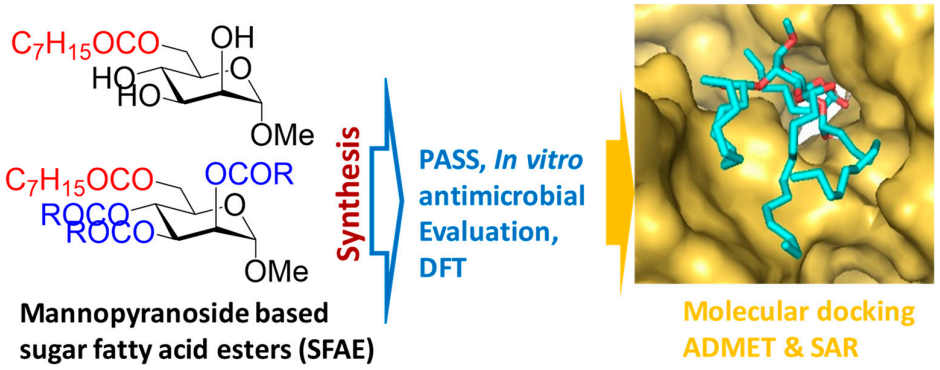

Abstract: The approval of sucrose fatty acid esters (SFAEs) as food additives/preservatives has triggered enormous interest in discovering new applications for these materials. Accordingly, many researchers reported that SFAEs consist of various sugar moieties, and hydrophobic side chains are highly active against certain fungal species. The combination of chain length and site of acylation is crucial in endowing the SFAE with high antimicrobial potency against *Aspergillus* species. Following several important studies, we herein present the synthesis and an assessment of the effects of acylation site and chain length (i.e., C-6 *vs.* C-2, C-3, C-4, and long-chain *vs.* short-chain) on the antimicrobial activity of mannopyranoside fatty acid esters. *In vitro* tests revealed that the fatty acid chain length in mannopyranoside esters significantly affects the antifungal activity where C12 chains are more potent against *Aspergillus* species. In terms of acylation site, mannopyranoside esters with a C8 chain substituted at the C-6 position are more active in antifungal inhibition. Molecular docking also revealed that these mannopyranoside esters had comparatively better stable binding energy, and hence better inhibition, with the fungal enzymes lanosterol 14-alpha-demethylase (3LD6), urate oxidase (1R51), and glucoamylase (1KUL) than the standard antifungal drug fluconazole. Additionally, the thermodynamic,

 doi:10.20944/preprints202311.0365.v1

orbital, drug-likeness, and safety profiles of these mannopyranoside esters were calculated and discussed, along with the structure-activity relationships (SAR). This study thus highlights the importance of the acylation site and lipid-like fatty acid chain length that govern the antimicrobial activity of mannopyranoside-based SFAE.

Keywords: ADMET; antimicrobial agents; effects of chain length; molecular docking; regioselective acylation; structure-activity relationship; sugar fatty acid ester (SFAE)

1. Introduction

Sugar fatty acid esters (SFAEs) are biobased surfactants widely used for the emulsification and dispersion of water-immiscible materials in organisms [1]. They are composed of a hydrophilic sugar moiety and one or more fatty acids as lipophilic moieties [2]. These molecules are generally tasteless, odorless, biodegradable, and non-toxic [3]. Since its approval as a food additive by the USFDA (21CFR 172.859), SFAE has triggered enormous interest in discovering new applications for these materials, such as antimicrobial [4–7], anticancer [8], insecticidal activities [9], and drug delivery [10–14]. There is no doubt that commercial sources of SFAE are available for various applications [15].

The use of synthetic SFAE, especially those enzymatically prepared monoesters, has been extensively investigated as antimicrobials [16]. Sucrose monolaurate and sucrose monocaprate, in particular, have been shown to inhibit the growth of several Gram-positive bacteria [5]. Mannopyranose monomyristate shows broad-spectrum inhibitory activity against a panel of bacteria and fungi, including methicillin-resistant *S. aureus* (MRSA) [17]. One of the proposed mechanisms of bacterial inhibition caused by these SFAEs was revealed through the disruption of the bacterial cell membrane, causing the release of intracellular components and subsequently rendering cell death [7]. The sugar moiety of these monoesters was found to have a significant effect on antimicrobial activity. Among the lauric esters of galactose, fructose, glucose, sucrose, and mannose, 6-*O*-lauroylgalactose showed the highest inhibitory effect against *S. mutans* [18]. Sucrose mononononanoate and lactose mononervonoate were found to selectively inhibit certain fungi such as *C. parapsilosis*, *E. faecalis*, *Y. enterocolitica*, and *C. albicans*, but not bacteria [19]. The potency of these sugar fatty acid monoesters has been proven, which opens new prospects for these compounds to be used as antimicrobials. While the majority of the antimicrobial studies have been focused on sugar fatty acid monoesters, relatively few studies have investigated sugar fatty acid diesters or oligoesters, mainly due to their low water solubility. 6-*O*-Methacryloylsucrose heptaacetate has been reported to inhibit a variety of clinical and food contaminant important microbial pathogens, with the lowest MIC of 0.28 μM [20]. Oligofatty acid esters of glucopyranoside and rhamnopyranoside have been shown to inhibit the growth of fungi *A. flavus*, *A. niger*, and yeast *C. albicans* at 10 μg/mL [21,22]. The issue of water solubility does not prevent the development of these high-order esters into antimicrobial agents. SFAE with low hydrophile-lipophile balance (HLB) values, i.e., low solubility, can be formulated in propylene glycol to enhance their penetration and absorption effects in transdermal drug delivery [10]. Other effective formulation strategies can also be applied to secure these compounds in the preclinical evaluation [23].

Methyl α-D-mannopyranoside (**1**) has been reported to prevent *E. coli* colonization and adherence [24]. Though some previous works have introduced the likelihood of using mannopyranoside or its derivatives as an antimicrobial, their application in antimicrobials has not been systematically studied [25]. Importantly, the lack of investigation into the structure-activity relationship (SAR) of mannopyranoside-based SFAE has impaired not only our understanding of SAFE–microbial interaction but also the development of more potent antimicrobial SFAE. Besides focusing on antimicrobial activity, the site of acylation, fatty acid chain length, and HLB are equally important contributing factors for microbial interactions, aqueous solubility, and membrane permeability [26]. Given that mannopyranoside-based SFAEs have the potential to enhance both antimicrobial inhibition and membrane permeability, various efforts have been made to enhance

Preprints (www.preprints.org) | NOT PEER-REVIEWED | Posted: 6 November 2023 doi:10.20944/preprints202311.0365.v1

their antimicrobial efficacy via the use of different types of fatty acids, e.g., of different alkyl chain lengths [27] and functional groups [28–30]. Very recently, we described the synthesis of 6-*O*-valeroyl-α-D-mannopyranosides that showed good efficacy against a panel of bacteria and fungi [31]. These SFAEs are essentially lipophilic, and we found that saturated valeric (C5) and caprylic (C8) chains were necessary to achieve good antimicrobial activity (Table 1).

Table 1. Antimicrobial potency of the recently reported sugar fatty acid esters.

Type of SFAE	SFAEs*	Active against	MIC	Ref.
monoester	6-*O*-lauroylsucrose	*Listeria monocytogenes*, *Bacillus subtilis*	2.5 mM	[7]
		Listeria monocytogenes, *Staphylococcus aureus*	0.4 mM	[32]
		Streptococcus suis	0.02 mg/mL	[33]
	6-*O*-myristoylsucrose	*Bacillus megaterium*	32 ng/mL	[34]
	6-*O*-caproylsucrose	*Bacillus cereus*, *Bacillus subtilis*, *Staphylococcus aureus*	2.5 mM	[5]
	6-*O*-nonanoylsucrose	*Candida parapsilosis*	0.313 mg/mL	[19]
	6-*O*-methacryloylsucrose	*Listeria monocytogenes*, *Micrococcus flavus*, *Enterobacter cloacae*, *E. coli*	0.24 μM	[20]
	6-*O*-nervonoyllactose	*Listeria monocytogenes*, *Escherichia coli*, *Staphylococcus enteritidis*, *Enterococcus faecalis*, *Yersinia enterocolitica*, *Candida albicans*	0.064 mg/mL	[6]
	6-*O*-lauroylmaltose	*Staphylococcus aureus*	0.25 mg/mL	[35]
	Methyl 6-*O*-lauroyl- α-D-glucopyranoside	*Staphylococcus aureus*, *Escherichia coli*, *Candida albicans*	0.188 mg/mL	[36]
	Methyl 6-*O*-lauroyl- β-D-glucopyranoside	*Staphylococcus aureus*	0.04 mM	[4]
	Methyl 6-*O*-lauroyl-α-D-mannopyranoside	*Staphylococcus aureus*	0.04 mM	[24]
oligoester	6-*O*-methacryloylsucrose heptaacetate	*Aspergillus versicolor*, *Penicillium funiculosum*, *Penicillium ochrochloron*	0.28 μM	[20]
	Octyl 2,4-di-*O*-decanoyl-3,6-di-*O*-valeroyl-β-D-glucopyranoside	*Escherichia coli*, *Aspergillus flavus*, *Aspergillus niger*, *Candida albicans*	68.4%	[22]
	Benzyl 4-*O*-benzoyl- α-L-rhamnopyranoside	*Candida albicans*	65.0%	[21]
	Methyl 2,3,4-tri-*O*-lauroyl-6-*O*- octanoyl-α-D-mannopyranoside	*Aspergillus flavus*, *Aspergillus niger*	58.2%	This work

*SFAEs = Sugar fatty acid esters; MIC = Minimum inhibitory concentration.

Here, we report an investigation of the acylation site and fatty acid chain length that affect the antimicrobial activity of mannopyranoside esters. For this study, mannopyranoside esters with various fatty acids substituted at C-2, C-3, C-4, and C-6 acylation sites are regioselectively synthesized. Their antimicrobial activities are evaluated against a panel of bacteria and fungi. Molecular docking and dynamics simulation are performed for the most active compound in the catalytic triad of putative targets (3LD6, 1R51, and 1KUL). *In silico* ADME prediction is carried out to analyze the therapeutic potential of these compounds as antimicrobials. Drug-likeness and safety profiles of the mannopyranoside esters are discussed, along with the structure-activity relationship (SAR).

 doi:10.20944/preprints202311.0365.v1

2. Materials and Methods

2.1. General methods

Evaporations were conducted below 40 °C under low pressure. Thin-layer chromatography (TLC) was performed on the Kieselgel GF_{254} plate and column chromatography (CC) was performed with Merck 230–400 mesh silica gel. The solvent system employed for the TLC and CC was chloroform/methanol and/or *n*-hexane/ethyl acetate in different ratios. FT-IR spectra were recorded on an FT-IR spectrophotometer (Shimadzu, IR Prestige-21) in the $CHCl_3$ technique. ^1H (400 MHz, Bruker DPX-400 spectrometer, Switzerland) and ^{13}C (100 MHz) NMR spectra were recorded in $CDCl_3$ solution. Chemical shifts were reported in δ unit (ppm) concerning tetramethylsilane as an internal standard and *J* values are shown in Hertz (Hz). Elemental analyses were conducted with CH-analyzer. Methyl α-D-mannopyranoside, ethanoic anhydride (acetic anhydride), acyl halides, etc. were purchased from Sigma-Aldrich (purity ≥99.0%).

2.2. Synthesis

Methyl 6-O-octanoyl-α-D-mannopyranoside (**2**). To a cooled (0 °C) mixture of methyl α-D-mannopyranoside (**1**) (1.0 g, 5.150 mmol) and anhydrous pyridine (3 mL) was added octanoyl chloride (0.801 g, 4.924 mmol) slowly. It was stirred at 0 °C for 8 h and then 6 h at room temperature when TLC indicated the conversion of the starting compound into a faster-moving single product (R_f = 0.43; chloroform/methanol = 5/1, v/v) with little starting material. The reaction was quenched with water. Usual workup followed by concentration and column chromatography purification provided compound **2** (1.004 g, 61%) as semi-solid which resisted crystallization. R_f = 0.43 (chloroform/methanol = 5/1); FT-IR ($CHCl_3$) ν_{max} (cm^{-1}): 3200-3550 (br, 3H, OH), 1732 (CO), 1062 cm^{-1} (pyranose ring); ^1H NMR (400 MHz, $CDCl_3$) δ ppm: 4.70 (s, 1H, H-1), 4.39 (dd, *J* = 12.2 and 5.0 Hz, 1H, H-6), 4.29 (dd, *J* = 12.2 and 1.2 Hz, 1H, H-6′), 3.95 (app d, *J* = 2.0 Hz, 1H, H-2), 3.78 (dd, *J* = 9.6 and 3.6 Hz, 1H, H-3), 3.67-3.73 (m, 1H, H-5), 3.62 (t, *J* = 9.6 Hz, 1H, H-4), 3.36 (s, 3H, OCH_3), 2.30-2.40 [m, 2H, $CH_3(CH_2)_5CH_2CO$], 1.58-1.67 (m, 2H, $CH_3(CH_2)_4CH_2CH_2CO$), 1.22-1.37 [br m, 8H, $CH_3(CH_2)_4(CH_2)_2CO$], 0.87 [t, *J* = 6.4 Hz, 3H, $CH_3(CH_2)_6CO$]; ^{13}C NMR (100 MHz, $CDCl_3$) δ ppm: 174.6 [$CH_3(CH_2)_6CO$], 100.9 (C-1), 71.5, 70.5, 70.5, (C-2/C-3/C-5), 67.7 (C-4), 64.0 (C-6), 54.8 (OCH_3), 34.2 [$CH_3(CH_2)_5CH_2CO$], 31.8 [$CH_3(CH_2)_4CH_2CH_2CO$], 29.1, 28.9 [$CH_3(CH_2)_2(CH_2)_2(CH_2)_2CO$], 24.9 [$CH_3CH_2CH_2(CH_2)_4CO$], 22.6 [$CH_3CH_2(CH_2)_5CO$], 14.0 [$CH_3(CH_2)_6CO$]; Anal. ($C_{15}H_{28}O_7$): C, 56.23; H, 8.81, Found: C, 56.25; H, 8.86.

General procedure for the syntheses of mannopyranoside esters 3–8. To a stirred solution of the **2** (0.1 g) in anhydrous pyridine (1 mL) was added the corresponding acyl halide (3.3 eq.) slowly at 0 °C, followed by the addition of a catalytic amount of *N*,*N*-dimethylpyridin-4-amine (DMAP, 0.01 g). The reaction mixture was allowed to reach room temperature and stirring was continued for 11-17 h. For compounds **6–8**, the reaction mixture was stirred for an additional 1-2 h at 45 °C prior to stopping the reaction. A small amount of ice was added to the reaction mixture to decompose excessive acyl halide, and the reaction mixture was extracted with dichloromethane (5×3 mL). The organic layer was washed successively with 5% hydrochloric acid, saturated aqueous sodium hydrogen carbonate solution, and brine. The organic layer was dried and concentrated under reduced pressure. The residue was purified using silica gel column chromatography (elution with *n*-hexane/ethyl acetate) and furnished with the corresponding targets.

Methyl 2,3,4-tri-O-acetyl-6-O-octanoyl-α-D-mannopyranoside (***3***). Clear syrup; yield 94%; R_f = 0.48 (*n*-hexane/EA = 4/1); FT-IR ($CHCl_3$) ν_{max} (cm^{-1}): 1748, 1741, 1738, 1735 (CO), 1084 (pyranose ring); ^1H NMR (400 MHz, $CDCl_3$) δ ppm: 5.26-5.37 (m, 3H, H-2, H-3 and H-4), 4.73 (d, *J* = 1.6 Hz, 1H, H-1), 4.26 (dd, *J* = 12.0 and 5.2 Hz, 1H, H-6), 4.17 (dd, *J* = 12.0 and 2.0 Hz, 1H, H-6′), 3.98 (ddd, *J* = 8.8, 5.2 and 2.0 Hz, 1H, H-5), 3.43 (s, 3H, OCH_3), 2.38 [t, *J* = 7.6 Hz, 2H, $CH_3(CH_2)_5CH_2CO$], 2.16 (s, 3H, CH_3CO), 2.05 (s, 3H, CH_3CO), 2.00 (s, 3H, CH_3CO), 1.59-1.71 [m, 2H, $CH_3(CH_2)_4CH_2CH_2CO$], 1.23-1.39 [m, 8H, $CH_3(CH_2)_4(CH_2)_2CO$], 0.89 [t, *J* = 6.8 Hz, 3H, $CH_3(CH_2)_6CO$]; ^{13}C NMR (100 MHz, $CDCl_3$) δ ppm: 173.5 [$CH_3(CH_2)_6CO$], 170.0, 169.9, 169.6 (CH_3CO), 98.6 (C-1), 69.6, 69.2, 68.5, (C-2/C-3/C-5), 66.2 (C-4), 62.4 (C-6), 55.3 (OCH_3), 34.1 [$CH_3(CH_2)_5CH_2CO$], 31.7 [$CH_3(CH_2)_4CH_2CH_2CO$], 29.1, 29.0 [$CH_3(CH_2)_2(CH_2)_2(CH_2)_2CO$], 24.8

 doi:10.20944/preprints202311.0365.v1

[$CH_3CH_2CH_2(CH_2)_4CO$], 22.6 [$CH_3CH_2(CH_2)_5CO$], 20.9, 20.7(2) (CH_3CO), 14.1 [$CH_3(CH_2)_4CO$]; Anal. ($C_{21}H_{34}O_{10}$): C, 56.49; H, 7.68; Found: C, 56.56; H, 7.73. The assignments of the signals were confirmed by scanning and analyzing its DEPT-135, COSY, HSQC, and HMBC experiments.

*Methyl 6-O-octanoyl-2,3,4-tri-O-pentanoyl-α-D-mannopyranoside (**4**)*. Semi-solid; yield 89%; R_f = 0.52 (*n*-hexane/EA = 4/1); FT-IR ($CHCl_3$) ν_{max} (cm^{-1}): 1754, 1749, 1745, 1739 (CO), 1082 (pyranose ring); ^1H NMR (400 MHz, $CDCl_3$) δ ppm: 5.38 (dd, *J* = 10.0 and 3.2 Hz, 1H, H-3), 5.33 (t, *J* = 10.0 Hz, 1H, H-4), 5.25-5.28(m, 1H, H-2), 4.72 (s, 1H, H-1), 4.25 (dd, *J* = 12.0 and 5.6 Hz, 1H, H-6), 4.16 (dd, *J* = 12.0 and 2.0 Hz, 1H, H-6′), 3.94-4.00 (m, 1H, H-5), 3.42 (s, 3H, OCH_3), 2.34-2.45, 2.27-2.32, 2.21-2.26 [3×m, 8H, $CH_3(CH_2)_5CH_2CO$ and $3\times CH_3(CH_2)_2CH_2CO$], 1.60-1.70, 1.50-1.59 [2×m, 8H, $CH_3(CH_2)_4CH_2CH_2CO$ and $3\times CH_3CH_2CH_2CH_2CO$], 1.23-1.42 [br m, 14H, $CH_3(CH_2)_4(CH_2)_2CO$ and $3\times CH_3CH_2(CH_2)_2CO$], 0.96, 0.90 [2×t, *J* = 7.2 Hz, 12H, $CH_3(CH_2)_6CO$ and $3\times CH_3(CH_2)_3CO$]; ^{13}C NMR (100 MHz, $CDCl_3$) δ ppm: 173.4, 172.8, 172.6, 172.4 [$CH_3(CH_2)_6CO$ and $3\times CH_3(CH_2)_3CO$], 98.7 (C-1), 69.3, 69.0, 68.6, (C-2/C-3/C-5), 65.8 (C-4), 62.4 (C-6), 55.3 (OCH_3), 34.1, 33.9, 33.8(2) [$CH_3(CH_2)_5CH_2CO$ and $3\times CH_3(CH_2)_2CH_2CO$], 31.7 [$CH_3(CH_2)_4CH_2CH_2CO$], 29.1, 29.0 [$CH_3(CH_2)_2(CH_2)_2(CH_2)_2CO$], 27.0, 26.9, 26.8 ($3\times CH_3CH_2CH_2CH_2CO$), 24.8 [$CH_3CH_2CH_2(CH_2)_4CO$], 22.6, 22.2(2), 22.1 [$CH_3CH_2(CH_2)_5CO$ and $3\times CH_3CH_2(CH_2)_2CO$], 14.1, 13.7, 13.6(2) [$CH_3(CH_2)_6CO$ and $3\times CH_3(CH_2)_3CO$]; Anal. ($C_{30}H_{52}O_{10}$): C, 62.91; H, 9.15; Found: C, 62.89; H, 9.18.

*Methyl 2,3,4-tri-O-hexanoyl-6-O-octanoyl-α-D-mannopyranoside (**5**)*. Oil; yield 82%; R_f = 0.54 (*n*-hexane/EA = 4/1); FT-IR ($CHCl_3$) ν_{max} (cm^{-1}): 1759, 1755, 1747, 1742, (CO), 1084 (pyranose ring); ^1H NMR (400 MHz, $CDCl_3$) δ ppm: 5.37 (dd, *J* = 10.0 and 2.8 Hz, 1H, H-3), 5.32 (t, *J* = 10.0 Hz, 1H, H-4), 5.26-5.28 (m, 1H, H-2), 4.72 (d, *J* = 1.1 Hz, 1H, H-1), 4.25 (dd, *J* = 12.0 and 5.6 Hz, 1H, H-6), 4.16 (dd, *J* = 12.0 and 1.8 Hz, 1H, H-6′), 3.96-4.01 (m, 1H, H-5), 3.42 (s, 3H, OCH_3), 2.35-2.45, 2.19-2.31 [2×m, 8H, $CH_3(CH_2)_5CH_2CO$ and $3\times CH_3(CH_2)_3CH_2CO$], 1.51-1.68 [m, 8H, $CH_3(CH_2)_4CH_2CH_2CO$ and $3\times CH_3(CH_2)_2CH_2CH_2CO$], 1.22-1.39 [br m, 20H, $CH_3(CH_2)_4(CH_2)_2CO$ and $3\times CH_3(CH_2)_2(CH_2)_2CO$], 0.87-0.95 [m, 12H, $CH_3(CH_2)_6CO$ and $3\times CH_3(CH_2)_4CO$]; ^{13}C NMR (100 MHz, $CDCl_3$) δ ppm: 173.4, 172.8, 172.6, 172.4 [$CH_3(CH_2)_6CO$ and $3\times CH_3(CH_2)_4CO$], 98.7 (C-1), 69.3, 69.0, 68.6, (C-2/C-3/C-5), 65.9 (C-4), 62.4 (C-6), 55.3 (OCH_3), 34.1 (4) [$CH_3(CH_2)_5CH_2CO$ and $3\times CH_3(CH_2)_3CH_2CO$], 31.7, 31.2(3) [$CH_3(CH_2)_4CH_2CH_2CO$ and $3\times CH_3(CH_2)_2CH_2CH_2CO$], 29.1, 29.0 [$CH_3(CH_2)_2(CH_2)_2(CH_2)_2CO$], 24.8, 24.6, 24.5, 24.4 [$CH_3CH_2CH_2(CH_2)_4CO$ and $3\times CH_3CH_2CH_2(CH_2)_2CO$], 22.6, 22.3(3) [$CH_3CH_2(CH_2)_5CO$ and $3\times CH_3CH_2(CH_2)_3CO$], 14.1, 14.0, 13.9(2) [$CH_3(CH_2)_6CO$ and $3\times CH_3(CH_2)_4CO$]; Anal. ($C_{33}H_{58}O_{10}$): C, 64.47; H, 9.51; Found: C, 64.54; H, 9.57.

*Methyl 2,3,4-tri-O-decanoyl-6-O-octanoyl-α-D-mannopyranoside (**6**)*. Semi-solid; yield 85%; R_f = 0.57 (*n*-hexane/EA = 4/1); FT-IR ($CHCl_3$) ν_{max} (cm^{-1}): 1755, 1747, 1745, 1740 (CO), 1084 (pyranose ring); ^1H NMR (400 MHz, $CDCl_3$) δ ppm: 5.36 (dd, *J* = 10.0 and 3.2 Hz, 1H, H-3), 5.33 (t, *J* = 10.0 Hz, 1H, H-4), 5.26 (dd, *J* = 3.4 and 1.2 Hz, 1H, H-2), 4.70 (s, 1H, H-1), 4.24 (dd, *J* = 12.2 and 5.6 Hz, 1H, H-6), 4.14 (dd, *J* = 12.2 and 1.6 Hz, 1H, H-6′), 3.95-3.99 (m, 1H, H-5), 3.41 (s, 3H, OCH_3), 2.32-2.42, 2.18-2.29 [2×m, 8H, $CH_3(CH_2)_5CH_2CO$ and $3\times CH_3(CH_2)_7CH_2CO$], 1.52-1.67 [m, 8H, $CH_3(CH_2)_4CH_2CH_2CO$ and $3\times CH_3(CH_2)_6CH_2CH_2CO$], 1.21-1.38 [br m, 44H, $CH_3(CH_2)_4(CH_2)_2CO$ and $3\times CH_3(CH_2)_6(CH_2)_2CO$], 0.89 [t, *J* = 6.8 Hz, 12H, $CH_3(CH_2)_6CO$ and $3\times CH_3(CH_2)_8CO$]; ^{13}C NMR (100 MHz, $CDCl_3$) δ ppm: 173.4, 172.8, 172.5, 172.4 [$CH_3(CH_2)_6CO$ and $3\times CH_3(CH_2)_8CO$], 98.6 (C-1), 69.3, 68.9, 68.6, (C-2/C-3/C-5), 65.8 (C-4), 62.4 (C-6), 55.2 (OCH_3), 34.2, 34.1(2), 33.9 [$CH_3(CH_2)_5CH_2CO$ and $3\times CH_3(CH_2)_7CH_2CO$], 31.8(3), 31.7 [$CH_3(CH_2)_4CH_2CH_2CO$ and $3\times CH_3(CH_2)_6CH_2CH_2CO$], 29.5, 29.4(2), 29.3(2), 29.2(3), 29.1(4), 29.0(2) [$CH_3(CH_2)_2(CH_2)_2(CH_2)_2CO$ and $3\times CH_3(CH_2)_2(CH_2)_4(CH_2)_2CO$], 25.0, 24.9, 24.8, 24.7 [$CH_3CH_2CH_2(CH_2)_4CO$ and $3\times CH_3CH_2CH_2(CH_2)_6CO$], 22.7(2), 22.6(2) [$CH_3CH_2(CH_2)_5CO$ and $3\times CH_3CH_2(CH_2)_7CO$], 14.1, 14.0(3) [$CH_3(CH_2)_6CO$ and $3\times CH_3(CH_2)_8CO$]; Anal. ($C_{45}H_{82}O_{10}$): C, 69.02; H, 10.55; Found: C, 69.05; H, 10.61.

*Methyl 2,3,4-tri-O-lauroyl-6-O-octanoyl-α-D-mannopyranoside (**7**)*. Syrup; yield 77%; R_f = 0.57 (*n*-hexane/EA = 4/1); FT-IR ($CHCl_3$) ν_{max} (cm^{-1}): 1752, 1747, 1745, 1739 (CO), 1082 (pyranose ring); ^1H NMR (400 MHz, $CDCl_3$) δ ppm: 5.36 (dd, *J* = 10.0 and 2.8 Hz, 1H, H-3), 5.32 (t, *J* =

 doi:10.20944/preprints202311.0365.v1

10.0 Hz, 1H, H-4), 5.27 (dd, *J* = 3.2 and 1.1 Hz, 1H, H-2), 4.71 (d, *J* = 1.1 Hz, 1H, H-1), 4.25 (dd, *J* = 12.4 and 5.6 Hz, 1H, H-6), 4.16 (dd, *J* = 12.4 and 2.0 Hz, 1H, H-6′), 3.96-4.00 (m, 1H, H-5), 3.42 (s, 3H, OC*H*$_3$), 2.35-2.44, 2.19-2.30 [2×m, 8H, CH$_3$(CH$_2$)$_5$C*H*$_2$CO and 3×CH$_3$(CH$_2$)$_9$C*H*$_2$CO], 1.51-1.69 [m, 8H, CH$_3$(CH$_2$)$_4$C*H*$_2$CH$_2$CO and 3×CH$_3$(CH$_2$)$_8$C*H*$_2$CH$_2$CO], 1.21-1.38 [br m, 56H, CH$_3$(C*H*$_2$)$_4$(CH$_2$)$_2$CO and 3×CH$_3$(C*H*$_2$)$_8$(CH$_2$)$_2$CO], 0.90 [t, *J* = 6.8 Hz, 12H, C*H*$_3$(CH$_2$)$_6$CO and 3×C*H*$_3$(CH$_2$)$_{10}$CO]; ^{13}C NMR (100 MHz, CDCl$_3$) δ ppm: 173.4, 172.8, 172.5, 172.4 [CH$_3$(CH$_2$)$_6$CO and 3×CH$_3$(CH$_2$)$_{10}$CO], 98.7 (C-1), 69.3, 68.9, 68.6, (C-2/C-3/C-5), 65.9 (C-4), 62.4 (C-6), 55.32 (OCH$_3$), 34.2, 34.1(2) [CH$_3$(CH$_2$)$_5$CH$_2$CO and 3×CH$_3$(CH$_2$)$_9$CH$_2$CO], 31.9 (3), 31.7 [CH$_3$(CH$_2$)$_4$CH$_2$CH$_2$CO and 3×CH$_3$(CH$_2$)$_8$CH$_2$CH$_2$CO], 29.6(5), 29.5(4), 29.4(2), 29.3(4), 29.1(3), 29.0(2) [CH$_3$(CH$_2$)$_2$(*C*H$_2$)$_2$(CH$_2$)$_2$CO and 3×CH$_3$(CH$_2$)$_2$(CH$_2$)$_6$(CH$_2$)$_2$CO], 25.0, 24.9, 24.8(2) [CH$_3$CH$_2$*C*H$_2$(CH$_2$)$_4$CO and 3×CH$_3$CH$_2$*C*H$_2$(CH$_2$)$_8$CO], 22.7(3), 22.6 [CH$_3$CH$_2$(CH$_2$)$_5$CO and 3×CH$_3$*C*H$_2$(CH$_2$)$_9$CO], 14.1(4) [*C*H$_3$(CH$_2$)$_6$CO and 3×*C*H$_3$(CH$_2$)$_{10}$CO]; Anal. (C$_{51}$H$_{94}$O$_{10}$): C, 70.63; H, 10.92; Found: C, 70.71; H, 10.96.

Methyl 6-O-octanoyl-2,3,4-tri-O-stearoyl-α-D-mannopyranoside (8). Semi-solid; yield 69%; *R*$_f$ = 0.66 (*n*-hexane/EA = 4/1); FT-IR (CHCl$_3$) ν$_{max}$ (cm^{-1}): 1751, 1747(3) (CO), 1084 (pyranose ring); ^{1}H NMR (400 MHz, CDCl$_3$) δ ppm: 5.36 (dd, *J* = 10.0 and 3.2 Hz, 1H, H-3), 5.32 (t, *J* = 10.0 Hz, 1H, H-4), 5.27 (d, *J* = 3.2 Hz, 1H, H-2), 4.71 (s, 1H, H-1), 4.25 (dd, *J* = 12.0 and 5.6 Hz, 1H, H-6), 4.15 (dd, *J* = 12.0 and 1.2 Hz, 1H, H-6′), 3.95-4.00 (m, 1H, H-5), 3.42 (s, 3H, OC*H*$_3$), 2.35-2.44, 2.18-2.29 [2×m, 8H, CH$_3$(CH$_2$)$_5$C*H*$_2$CO and 3×CH$_3$(CH$_2$)$_{15}$C*H*$_2$CO], 1.53-1.69 [m, 8H, CH$_3$(CH$_2$)$_4$C*H*$_2$CH$_2$CO and 3×CH$_3$(CH$_2$)$_{14}$C*H*$_2$CH$_2$CO], 1.21-1.38 [br m, 92H, CH$_3$(C*H*$_2$)$_4$(CH$_2$)$_2$CO and 3×CH$_3$(C*H*$_2$)$_{14}$(CH$_2$)$_2$CO], 0.90 [t, *J* = 7.2 Hz, 12H, C*H*$_3$(CH$_2$)$_6$CO and 3×C*H*$_3$(CH$_2$)$_{16}$CO]; ^{13}C NMR (100 MHz, CDCl$_3$) δ ppm: 173.4, 172.8, 172.5, 172.4 [CH$_3$(CH$_2$)$_6$CO and 3×CH$_3$(CH$_2$)$_{16}$CO], 98.7 (C-1), 69.3, 69.0, 68.6, (C-2/C-3/C-5), 65.8 (C-4), 62.4 (C-6), 55.2 (OCH$_3$), 34.2, 34.1(3) [CH$_3$(CH$_2$)$_5$CH$_2$CO and 3×CH$_3$(CH$_2$)$_{15}$CH$_2$CO], 31.9(3), 31.7 [CH$_3$(CH$_2$)$_4$CH$_2$CH$_2$CO and 3×CH$_3$(CH$_2$)$_{14}$CH$_2$CH$_2$CO], 29.7(12), 29.6(10), 29.5(2), 29.4, 29.3(4), 29.3(5), 29.1(3), 29.0 [CH$_3$(CH$_2$)$_2$(*C*H$_2$)$_2$(CH$_2$)$_2$CO and 3×CH$_3$(CH$_2$)$_2$(CH$_2$)$_{12}$(CH$_2$)$_2$CO], 25.0, 24.9, 24.8(2) [CH$_3$CH$_2$CH$_2$(CH$_2$)$_4$CO and 3×CH$_3$CH$_2$CH$_2$(CH$_2$)$_{14}$CO], 22.7(3), 22.6 [CH$_3$CH$_2$(CH$_2$)$_5$CO and 3×CH$_3$CH$_2$(CH$_2$)$_{15}$CO], 14.1(3), 14.0 [*C*H$_3$(CH$_2$)$_6$CO and 3×*C*H$_3$(CH$_2$)$_{16}$CO]; Anal. (C$_{69}$H$_{130}$O$_{10}$): C, 74.01; H, 11.70; Found: C, 74.05; H, 11.68. The assignments of the signals of **8** were established by scanning and analyzing its DEPT-135, COSY, HSQC, and HMBC experiments.

2.3. Prediction of Activity Spectra for Substances (PASS)

For the web-based prediction of PASS, structures of the compounds were drawn and then converted into their SMILES (simplified molecular-input line-entry system). These SMILES were used to predict biological spectrum using the PASS online version (http://www.way2drug.com/passonline/).

2.4. Evaluation of in vitro antimicrobial activities

Two Gram-positive (*Bacillus cereus* BTCC 19 and *Bacillus subtilis* ATCC 6633) and two Gram-negative (*Escherichia coli* ATCC 25922 and *Salmonella typhi* AE 14612) bacteria were tested by using the CLSI standardized disc diffusion method [38]. *In vitro* antifungal activities were investigated against *Aspergillus flavus*, *Aspergillus niger*, *Fusarium equiseti*, and *Penicillium notatum* [39]. The test tube cultures of the bacterial and fungal pathogens were collected from the Biochemistry Laboratory, Department of Biochemistry and Molecular Biology, University of Chittagong, Bangladesh. Proper control was maintained without chemicals. Each experiment was carried out three times. All the results were compared with the standard antibacterial antibiotic ampicillin (brand name Avlocillin, ACI Ltd., Bangladesh) and antifungal antibiotic fluconazole (brand name Omastin, Beximco Pharmaceuticals Ltd., Bangladesh).

Preprints (www.preprints.org) | NOT PEER-REVIEWED | Posted: 6 November 2023 doi:10.20944/preprints202311.0365.v1

2.5. Computational method for molecular docking

Preparation of protein: The starting three-dimensional (3D) structure of different fungi from the RCSB Protein Data Bank (PDB) https://www.rcsb.org/. The lanosterol 14α-demethylase was taken from PDB which was uploaded and consist of Glucoamylase. The *Aspergillus flavus* (1R51), *Aspergillus niger* (1kul), *Aspergillus aculeatus* (1IA5), were taken from PDB as the pdb type of file. After taking the protein from RCSB Protein Data Bank (PDB; https://www.rcsb.org/), it was inputted Pymol software version using PyMOL V2.3 (https://pymol.org/2/). The input files in PyMOL software identified the protein, ligands, and water molecules, and then it was saved as PDB files [40–42].

Preparation of ligands: For the preparation of ligands, Gaussian 09 was used. At first, the ligand molecules were drawn by GaussView (5.0) and input into Gaussian 09 software for its optimization. For optimization, the density functional method (DFT) was used for simulation and saving in PDB form.

Molecular docking: For molecular docking, PyRx software was used. Although it consists of Auto Dock 4 and Auto Dock Vina, we have used Auto Dock Vina only and is found more sophisticated than others for calculating binding energy and docking site with non-polar and polar bonds. Initially, the PyRx was opened and uploaded the macromolecules as proteins for simulating [42]. Then opened the bubal and uploaded the ligand and optimized minimum energy. Using Auto Dock Vina, the docking was performed by selecting the active site of the protein. Maximum grid box size was X = 61.8544, Y = 61.6556, Z = 70.6697 Å for 13LD6; X = 58.4699, Y = 70.0953, Z = 58.3121 Å for 1R51; X = 36.9822, Y = 48.2899, Z = 31.8335 Å for 1KUL; and X = 67.8720, Y = 51.2189, Z = 42.0505 Å for 1IA5. After finishing the job, it was saved as win rar files.

2.6. DFT calculations

For the DFT (density functional theory) calculations, the basic geometry of methyl α-D-mannopyranoside (**1**) was taken from the online structure database (ChemSpider). Then the other CFA esters **2-8** were drawn in GaussView (5.0) program. All these compounds were optimized using Gaussian 09 program at B3LYP/6-31G* basis set of DFT. HOMO (highest occupied molecular orbital) and LUMO (lowest unoccupied molecular orbital) gap, hardness (η), and softness (S) were calculated at the same level of theory using the following equations [43]:

Gap = [εLUMO - εHOMO]; $\eta = \frac{\varepsilon LUMO - \varepsilon HOMO}{2}$; $S = \frac{1}{\eta}$

To visualize MEP online WebMO demo server was used and a DOS plot was drawn from GaussSum 3.0.

2.7. Hydrophile-lipophile balance (HLB) calculation

HLB values were calculated using Grifin's method of non-ionic surfactants [44].

Grifin's mathematical method = 20×(MH/M)

MH = molecular weight of the hydrophilic group.

M = molecular weight of the whole molecule.

2.8. ADMET analysis

Absorption, distribution, metabolism, excretion and toxicity (ADMET) analyses were conducted by using computational approaches. At first all the structures of MDM esters were drawn in ChemDraw 16.0 to collect InChI Key, isomeric SMILES and SD file format. ADMET of all the MDM esters were predicted by using AdmetSAR [45] and SwissADME [46] free web tools. SMILES (simplified molecular-input line-entry system) strings were used throughout the process.

Preprints (www.preprints.org) | NOT PEER-REVIEWED | Posted: 6 November 2023 doi:10.20944/preprints202311.0365.v1

3. Results and discussion

3.1. One-step regioselective octanoylation of mannopyranoside 1

Methyl *α*-D-mannopyranoside (MDM, **1**) was chosen for 6-*O*-octanoylation on purpose due to its expanding biological profile. Thus, treatment of MDM with equimolar octanoyl chloride at low temperature (0-22 °C) for 14 h formed a faster-moving 6-*O*-octanoate **2** (61%, Scheme 1) exerting regioselectivity at the C-6 hydroxyl position.

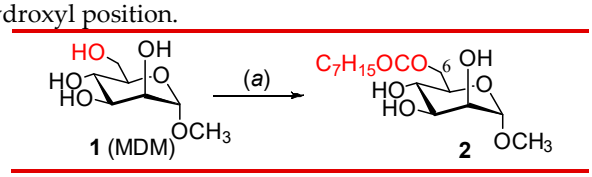

Scheme 1. *Reagents and conditions*: (*a*) dry pyridine, $C_7H_{15}COCl$, 0 °C, 8 h, rt, 6 h, 61%.

The FT-IR spectrum of this semi-solid showed characteristic resonance bands at 3200-3550 (br OH) and 1732 cm^{-1} (CO), indicating the partial attachment of an octanoyl group to the MDM molecule. In the ^1H NMR spectrum, two two-proton multiplets at δ 2.30-2.40 and 1.58-1.67, an eight-proton broad multiplet at δ 1.22-1.37, and a three-proton triplet at δ 0.87 (*J* 6.4 Hz) indicated the attachment of only one octanoyloxy group in the molecule. Furthermore, corresponding H-6 (δ 4.39) and H-6′ (δ 4.29) resonated considerably downfield as compared to its precursor MDM [37] clearly demonstrating the incorporation of octanoyloxy group at the C-6 position of the molecule. Additional analysis of its ^{13}C NMR spectrum and elemental analyses led us to assign the compound as methyl 6-*O*-octanoyl-*α*-D-mannopyranoside (**2**).

To improve the yield, the reaction was conducted with several solvents and catalysts (Table 2). Most of them formed inseparable complex mixtures, and mono-substituted ester yield was low. Only the conditions of (*i*) using a bulkier acylating agent like octanoyl chloride, (*ii*) using an exactly equimolar reagent or less than that, and (*iii*) using a lower temperature (0 °C) led to better yields.

Table 2. Different reaction conditions for the selective 6-*O*-substitution of **1**.

Entry	Reagent ($C_7H_{15}COCl$) (equivalent)	Solvent	Catalyst	Temperature (°C)	Product	Yield (2) %
1.	1.2	pyridine	-	0 - 25	**4** & mixture[a]	37
2.	0.98	pyridine	-	0 - 22	**4** & mixture	61
3.	0.98	pyridine	DMAP	0 - 22	**4** & mixture	49
4.	1.1	Pyridine & $CHCl_3$	-	0 - 22	**4** & mixture	43
5.	1.1	Pyridine & $CHCl_3$	DMAP	0 - 22	**4** & mixture[b]	33
6	1.1	$CHCl_3$	DMAP	0 - 22	**4** & mixture[b]	39

[a]Inseparable mixture of di- and tri-substituted products; [b]Starting recovered.

3.2. Synthesis of 2,3,4-tri-O-acylates of 6-O-octanoate 2

In an attempt to get newer ester derivatives of **2**, we have synthesized six 2,3,4-tri-*O*-acyl esters of various chain lengths (C2-C18) employing acetic anhydride, pentanoyl chloride, hexanoyl chloride, decanoyl chloride, lauroyl chloride, and stearoyl chloride. Initially, 2,3,4-triol **2** on reaction with acetic anhydride in pyridine in the presence of DMAP (cat.) for 11 h afforded a faster-moving single product in 94% (Scheme 2). In its FT-IR spectrum, four carbonyl stretching peaks were observed at 1748, 1741, 1738, and 1735 cm^{-1}, and the disappearance of an OH group frequency indicated the tri-*O*-acetylation of the molecule. In its ^1H NMR spectrum, three three-proton singlets at δ 2.16, 2.05, and 2.00 were assigned for acetyloxy-methyl protons. The H-2, H-3, and H-4 protons appeared considerably downfield at δ 5.26-5.37 as multiplets as compared to δ 3.95, 3.78, and 3.62,

Preprints (www.preprints.org) | NOT PEER-REVIEWED | Posted: 6 November 2023 doi:10.20944/preprints202311.0365.v1

respectively of its precursor **2**, and hence clearly indicated the attachment of acetyloxy groups at the C-2, C-3, and C-4 positions, respectively. Three acetyl carbonyl peaks appeared in its ^{13}C NMR at δ 170.0, 169.9, and 169.6; additionally, three acetyl methyl carbons resonated at δ 20.9 and 20.7(2). Based on its FT-IR, ^{1}H, and ^{13}C NMR data, the structure was assigned as methyl 2,3,4-tri-*O*-acetyl-6-*O*-octanoyl-*α*-D-mannopyranoside (**3**).

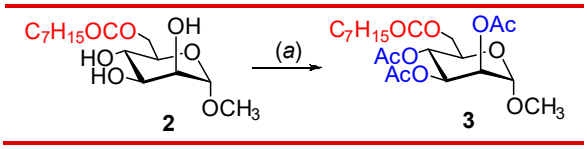

Scheme 2. *Reagents and conditions*: (*a*) Py, Ac_2O, DMAP, 0 °C-rt, 11 h, 94%.

The assignments of the signals for compound **3** were also confirmed by scanning, and analyzing its DEPT-135, 2D COSY, HSQC, and HMBC experiments. For example, the positions of three $COCH_3$ groups at C-2, C3, and C-4 positions and one COC_7H_{15} group at C-6 in the HMBC experiment are shown in Figure 1.

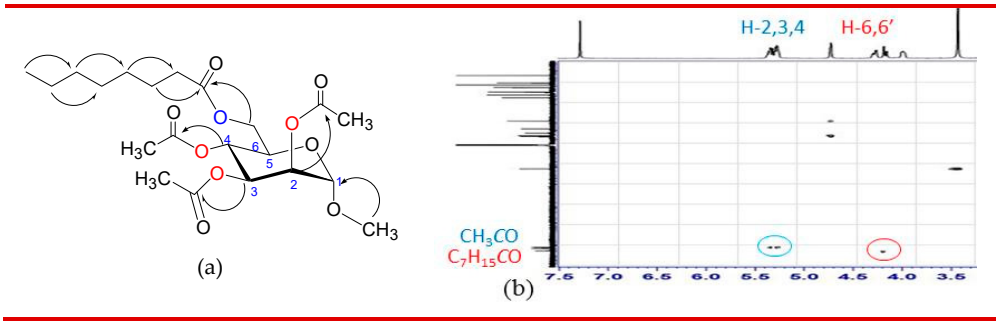

Figure 1. The HMBC correlations for (*a*) the compound **3** and (*b*) *C*O groups.

Successful synthesis and characterization of the tri-*O*-acetate **3** led us to use more aliphatic acyl halides for the derivatization of **2**. Thus, the reaction of compound **2** with excess pentanoyl chloride and hexanoyl chloride, separately followed by purification furnished 2,3,4-tri-*O*-pentanoate **4** and 2,3,4-tri-*O*-hexanoate **5**, respectively in good yields (Scheme 3). All these compounds were well characterized by FT-IR, ^{1}H, and ^{13}C NMR spectra.

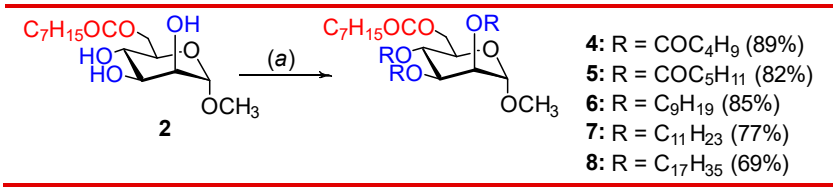

Scheme 3. *Reagents and conditions*: (*a*) Py, RCOCl, DMAP, 0 °C-rt, 13-15 h, 45 °C, 1-2 h.

Finally, we used three higher fatty acid halides, such as decanoyl chloride, lauroyl chloride, and stearoyl chloride, for the derivatization of **2** (Scheme 3). In these reactions, 2,3,4-tri-*O*-decanoate **6**; 2,3,4-tri-*O*-laurate **7**; and 2,3,4-tri-*O*-stearate **8**, respectively were obtained with reasonably good yields. All the structures were established by spectroscopic analyses as well as correlation with other MDM tri-*O*-acyl esters (**3**-**5**). The structure of compound **8** and the assignment of signals were completely supported by its DEPT-135, COSY, HSQC, and HMBC spectra. Thus, we have successfully synthesized 6-*O*-octanoate and its six acyl esters with the MDM core skeleton employing the direct acylation technique with various fatty acid-derived acylating reagents (C2-C18).

Preprints (www.preprints.org) | NOT PEER-REVIEWED | Posted: 6 November 2023 doi:10.20944/preprints202311.0365.v1

3.3. Computational-based biological activity evaluation

Recognized essential pharmacological and toxicological activities of a compound can be predicted simultaneously by the web-based PASS (prediction of activity spectra for substances) program with 90% accuracy in a non-laborious and inexpensive way [47]. The results are presented as Pa (probability for active compound) and Pi (probability for inactive compound) where Pa>Pi is considered possible for a particular compound, and their values vary from 0.000 to 1.000. In the present study, PASS results for antibacterial, antifungal, anticarcinogenic, and antioxidant properties are mentioned in Table 3.

Table 3. Predicted biological activity of synthesized MDM esters **2-8** using PASS software.

Drugs	Biological activity							
	Antibacterial		Antifungal		Anticarcinogenic		Antioxidant	
	Pa*	Pi	Pa	Pi	Pa	Pi	Pa	Pi
3	0.528	0.014	0.669	0.012	0.731	0.008	0.667	0.004
4	0.558	0.012	0.675	0.011	0.769	0.010	0.530	0.008
5	0.551	0.012	0.673	0.011	0.675	0.010	0.461	0.008
6	0.551	0.012	0.673	0.011	0.614	0.012	0.461	0.008
7	0.551	0.012	0.673	0.011	0.614	0.012	0.461	0.008
8	0.551	0.012	0.673	0.011	0.614	0.012	0.461	0.008
9	0.551	0.012	0.673	0.011	0.614	0.012	0.463	0.008
10	0.551	0.012	0.673	0.011	0.614	0.012	0.463	0.008

*Pa = Probability 'to be active'; Pi = Probability 'to be inactive'.

PASS predication clearly indicated 0.52<Pa<0.55 for antibacterial and 0.67<Pa<0.68 for antifungal (Table 3). Thus, the MDM esters **2-8** had more potentiality against phytopathogenic fungi as compared to those bacterial pathogens. The prediction was also extended for anticarcinogenic and antioxidant evaluation (Table 3) where 0.61<Pa<0.77 was observed for anticarcinogenic and 0.46<Pa<0.67 for antioxidant. The results thus indicated that the esters **2-8** were more potent as anticarcinogenic agents than their antioxidant properties, and hence, needed further studies to validate these promising results.

3.4. In vitro antimicrobial evaluation of MDM esters

The *in vitro* antimicrobial activity of the MDM esters was evaluated against four bacterial and four fungal pathogens.

Effects of MDM esters 2-8 against bacteria. For antibacterial tests, two Gram-positive, and two Gram-negative organisms were used and evaluated by the disc diffusion method [48]. Gram-positive organisms were *Bacillus cereus* BTCC 19, and *Bacillus subtilis* BTCC 17. Two Gram-negative organisms were *Escherichia coli* ATCC 25922, and *Salmonella typhi* AE 14612. The results in the form of inhibition zone (diameter) due to the effect of synthesized CFA esters **2-8** are presented in Table 4, and Figure 2, which indicated that these CFA esters were weak to moderate inhibitors against both of these tested Gram-positive and Gram-negative pathogens.

Table 4. Inhibition on bacterial pathogens by MDM esters.

Drug	Diameter of zone of inhibition in mm (100 µg dw / disc)			
	B. cereus	*B. subtilis*	*E. coli*	*S. typhi*
1	NI	NI	NI	NI
2	6.17±0.29	*10.27±0.46	NI	7.17±0.29
3	8.00±0.50	*10.67±0.58	6.50±0.40	NI
4	*12.33±0.58	7.00±0.40	7.00±00	8.00±0.30
5	6.17±0.29	8.00±1.00	NI	*10.50±0.50
6	6.50±0.50	NI	7.00±1	8.00±0.35

Preprints (www.preprints.org) | NOT PEER-REVIEWED | Posted: 6 November 2023 doi:10.20944/preprints202311.0365.v1

7	6.50±0.50	NI	7.17±0.29	*10.73±0.46
8	7.00±1.00	7.00±0.20	7.50±0.5	8.00±0.00
Ampicillin**	*10.60±0.53	*12.67±0.58	*15.54±0.5	*13.23±0.41

Data are presented as (Mean±SD). Values are represented for the triplicate of all the experiments. Significant inhibition values are marked with * sign for test compounds and, ** sign for reference antibiotic ampicillin (25 µg/disc). dw = Dry weight; NI = No inhibition. NI was observed for control DMF.

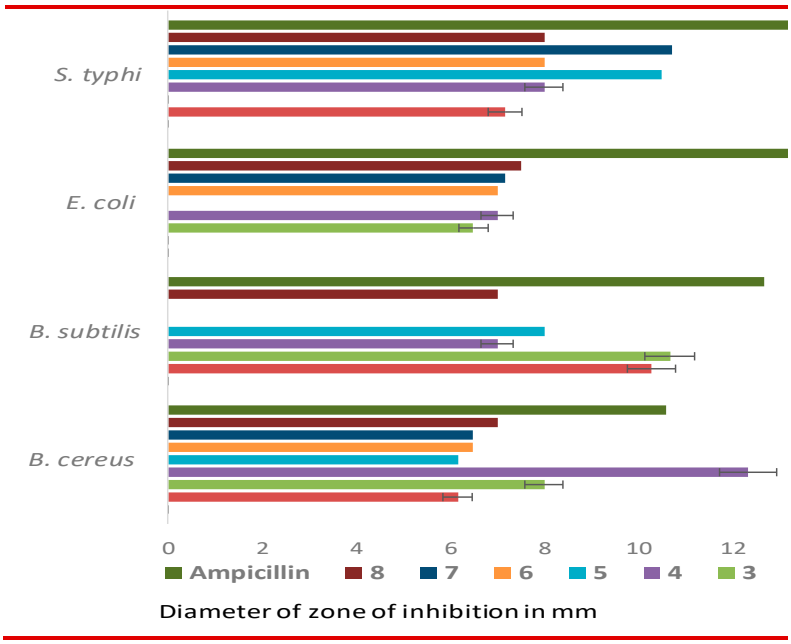

Figure 2. Activities against bacterial pathogens by **1**-**8**.

Effects of MDM esters 2-8 against fungal pathogens. The effect of the MDM esters **2**-**8** against four pathogenic fungi viz. *Aspergillus flavus*, *Aspergillus niger*, *Fusarium equiseti*, and *Penicillium notatum* are presented in Table 5, and Figure 3. The results are presented in the form of percentage inhibitions of mycelial growth [48,49].

Table 5. Inhibition of fungal pathogens by the MDM esters.

Drug	% Inhibition of fungal mycelial growth (100 µg dw / mL PDA)			
	A. flavus	*A. niger*	*F. equiseti*	*P. notatum*
1	NI	NI	NI	NI
2	NI	NI	*54.57±0.41	33.33±0.58
3	NI	40.23±0.25	NI	NI
4	NI	22.22±0.27	43.13±0.32	NI
5	22.22±0.26	NI	*59.37±0.55	38.27±0.40
6	9.53±0.45	NI	46.42±0.47	45.67±0.58
7	*58.33±0.58	*54.17±0.29	*54.93±0.76	28.20±0.26
8	NI	40.53±0.76	*52.00±0.72	38.50±0.50
**Fluconazole	47.03±0.25	37.10±0.17	*62.00±0.50	*65.73±0.46

Data are presented as (Mean±SD). Values are represented for the triplicate of all the experiments. Significant inhibition values are marked with * sign for test compounds, and ** sign for reference antibiotic fluconazole (12.5 µg/mL PDA). dw = Dry weight; NI = No inhibition; NI was observed for control DMF.

Preprints (www.preprints.org) | NOT PEER-REVIEWED | Posted: 6 November 2023 doi:10.20944/preprints202311.0365.v1

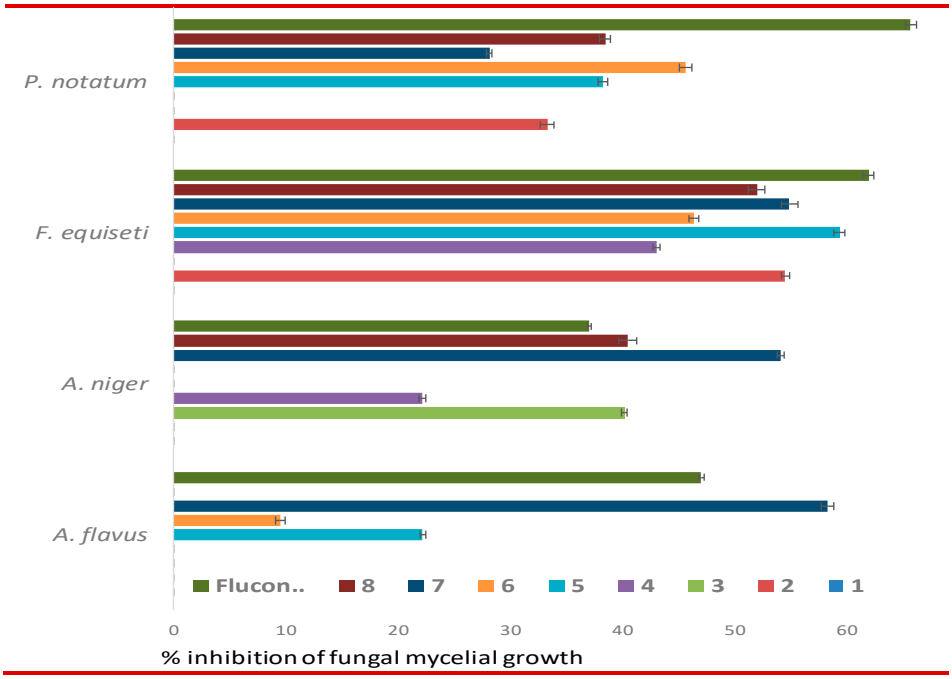

Figure 3. Activities on fungal pathogens by **1**-**8**.

It should be noted that MDM (**1**) didn't show any inhibition whereas the introduction of ester groups at different positions increased antifungal activities. MDM esters especially **5** (*59.37%), **7** (*54.93%), **2** (*54.57%), and **8** (*52.00%) were found more prone against *F. equiseti*, and comparable to standard antifungal antibiotic fluconazole (*62.00%). 6-*O*-Capryl-2,3,4-tri-*O*-lauroyl esters **7** exhibited better inhibition against *A. flavus* (58.33%) and *A. niger* (54.17%) which was higher than fluconazole (47.03% and 37.10%, respectively). Thus, most of the MDM-based CFA esters **2**–**8** possess excellent potentiality towards all tested fungal pathogens than the bacterial organisms. To our surprise, these *in vitro* results are in complete agreement with PASS predication results. Also, some compounds like **5**, **7**, and **8** exhibited encouraging antifungal and antibacterial potentiality which need further study to establish them as antifungal antibiotics.

3.5. Molecular docking and nonbonding interactions

With the encouraging antifungal results of several MDM esters, it was thought to investigate with molecular docking of compounds **2-8** with related fungal proteins essential for antifungal functionality. Especially, inhibition (binding) of lanosterol 14α-demethylase (3LD6/CYP51A1) is necessary for antifungal action [50]. For better explanation and comparison molecular docking of MDM (**1**), standard antifungal antibiotic fluconazole (FCZ), nystatin (NST), and papulacandin D (PCD), were calculated. For the SAR study, binding affinities were also calculated for caprylic acid (CA), lauric acid (LA), and stearic acid (SA), and are presented in Table 6, and Figure 4. Binding energy was calculated for lanosterol 14α-demethylase, and three fungi (Table 6).

Table 6. Molecular docking score (binding energy) of **1**-**8** and some important antibiotics.

Drugs/Compounds	Lanosterol 14α-demethylase (3LD6)	Fungi (kcal/mol)		
		A. flavus (1R51)	*A. niger* (1KUL)	*A. aculeatus* (1IA5)
1	-5.3	-5.4	-4.6	-4.3
2	-6.7	-6.3	-4.7	-5.2
3	-6.4	-6.3	-4.8	-6.7
4	-5.8	-6.1	-4.4	-6.2

Preprints (www.preprints.org) | NOT PEER-REVIEWED | Posted: 6 November 2023 doi:10.20944/preprints202311.0365.v1

5	-5.7	-5.6	-4.3	-5.8
6	-5.3	-5.7	-4.3	-5.4
7	-7.7	-7.1	-3.8	-4.1
8	-5.0	-5.1	-3.1	-4.9
FCZ*	-6.5	-7.0	-6.5	-5.4
NST	-5.6	-6.1	-4.6	-4.4
PCD	-8.9	-7.8	-6.4	-5.9
CA	-4.9	-4.7	-4.2	-3.9
LA	-5.0	-4.8	-4.3	-4.5
SA	-4.8	-5.3	-3.8	-5.0

* Fluconazole (FCZ), nystatin (NST), papulacandin D (PCD), ampicillin (APC) were used as standard drugs and to compare with CFA esters; Pymol software version using PyMOL V2.3 used for protein preparation; PyRx software was used for molecular docking; Discovery studio version 2017 was performed for analysis and view of docking result; Generally the binding energy is -6.0 to -8.5 kcal/mol for a good drug.

It was evident from Table 6 that mannopyranoside-based ester **7** with one caprylic chain (C8) and three lauric chains (C12) possess a binding affinity with 3LD6 (-7.7 kcal/mol), and with 1R51 (-7.1 kcal/mol) which was better than that of standard fluconazole (-6.5 and -7.0 kcal/mol, respectively). The binding energy of CA, LA, and SA was calculated to compare with that of CFA esters and standard antibiotics whether these hydrolysis products were responsible for inhibition activities or not. Although CA, LA, and SA showed some binding energy values with 3LD6, for three fungi (*A. flavus, A. niger*, and *A. aculeatus,*), the values were very much lower than those of FCZ, NST, and PCD. Also, in most of the cases, they showed lower binding affinity than those of mannopyranoside esters **2-8**. These observations indicated that CA, LA, and SA were not involved in the enzyme inhibition process.

Again, the interaction of drug molecules with various amino acid (AA) residues of the importance of lanosterol 14α-demethylase (3LD6) is also determined. It was found that MDM ester **7** interacts with several AAs *via* the formation of H-bonding, Pi-alkyl bonding, alkyl bond, and Pi-sigma bond similar to or even better than that of the standard antifungal drugs. MDM (**1**), CA, LA, and SA didn't show significant interactions with these AAs although LA has some van der Walls interactions. Better interaction is essential for the inhibition of the enzyme. To make it more visible binding affinity of **7** with the 3LD6 is also shown in 2D and 3D pose format as shown in Figure 4.

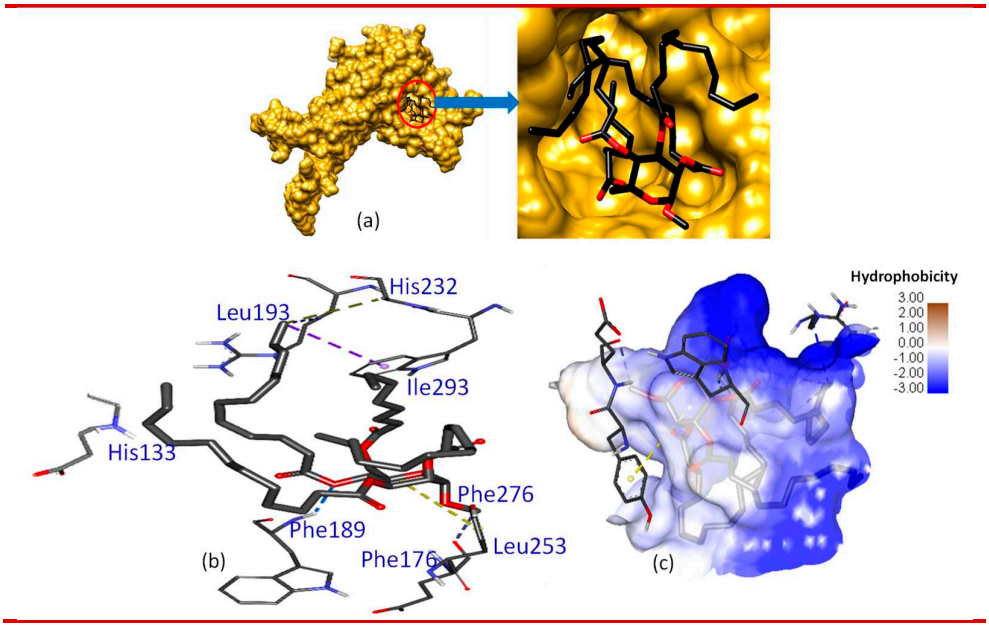

Preprints (www.preprints.org) | NOT PEER-REVIEWED | Posted: 6 November 2023 doi:10.20944/preprints202311.0365.v1

Figure 4. (*a*) Ligand **7** in binding pocket of 1R51 after docking; (*b*) Binding interactions of **7** with the active protein residues of urate oxidase (1R51); (*c*) 3D Hyrophobic representation of interaction between 1R51 and **7**. It should be noted that the long alkyl chain(s) of ester moieties in compounds **2**-**8** underwent bending during molecular docking.

3.6. DFT-based thermodynamic properties

DFT (density functional theory; B3LYP/6-31G* basis set) based optimized structure (298.15 K, 1.0 atm) of MDM **1**-**8** are presented in Figure 5. Also, thermodynamic properties such as RB3LYP electronic energy (EE), enthalpy (ΔH), Gibbs free energy (G), dipole moment (μ), total energy, and Van der Waals forces calculated at 298.15 K are shown in Table 7.

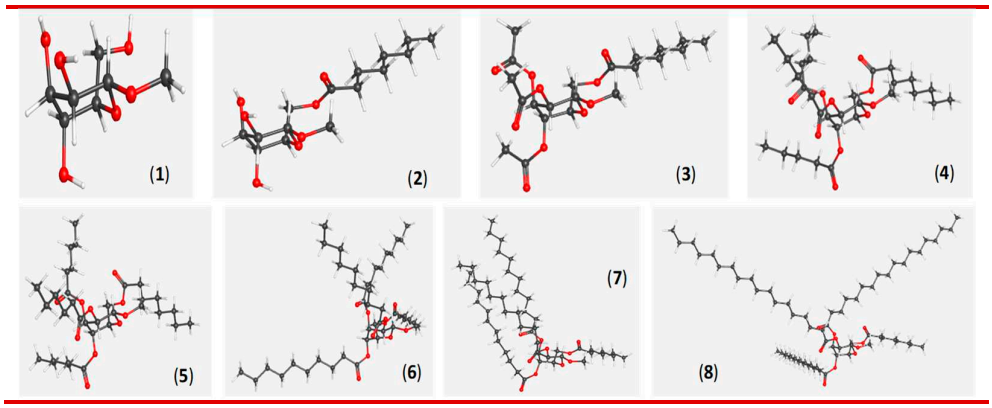

Figure 5. DFT optimized (B3LYP/6-31G*) structures of **2**-**8** (visualized from webMO).

Table 7. Physicochemical and thermodynamic properties of **1**-**8**.

Comp. No.	MF*	MW (g/mol)	RB3LYP, EE (Hartree)	ΔH (Hartree)	*G* (Hartree)	μ (Debye)	WebMO Mechanics	
							TE	VWE
1	$C_7H_{14}O_6$	194.18	-726.22423	-725.9849	-726.0398	3.3323	62.3786	44.0835
2	$C_{15}H_{28}O_7$	320.38	-1114.6733	-1114.2110	-1114.2941	2.9772	67.2912	43.0505
3	$C_{21}H_{34}O_{10}$	446.49	-1572.4892	-1571.9035	-1572.0140	8.4446	78.3025	60.8014
4	$C_{30}H_{52}O_{10}$	572.73	-1926.2212	-1925.3637	-1925.5067	7.1562	91.5670	59.2060
5	$C_{33}H_{58}O_{10}$	614.81	-2044.1349	-2043.1875	-2043.3400	6.5944	92.7009	64.1183
6	$C_{45}H_{82}O_{10}$	783.13	-2502.8194	-2501.5084	-2501.6961	6.1728	109.2732	83.0093
7	$C_{51}H_{94}O_{10}$	867.29	-2737.4306	-2735.9377	-2736.1367	7.5728	94.3915	56.8761
8	$C_{69}H_{130}O_{10}$	1119.76	-3441.2472	-3432.3005	-3432.5009	6.8291	127.6629	86.6837

*MF = molecular formula; TE = total energy (kcal/mol); VWE = van der Waals energy (kcal/mol).

All the compounds were found to possess almost regular $^4C_1$ conformation with C1 symmetry. Here, negative RB3LYP EE gradually increased with the increase of the number and chain length of the ester group(s) indicating the gradual increase of tightness of electron binding to the nucleus, and hence, stabilizes the molecules. Similarly, the negative value Gibbs free energy (*G*) also increases gradually with the increase of acyl group(s) to the MDM molecule where $G < 0$ signifies the spontaneity of a reaction [51,52]. These EE and *G* values agree with their exothermic esterification reactions, spontaneous binding, and interaction with other substrates. The ester compounds **2**-**8** had higher dipole moments than the non-ester precursor **1**, suggesting a higher binding affinity with the target enzyme during antimicrobial actions. WebMo molecular mechanics (https://www.webmo.net) indicated that lauroyl compound **7** had lower total energy (94.4 kcal/mol) and van der Waals energy (56.9 kcal/mol) compared to decanoate **6** and stearate **8** (Table 7). This clearly indicated the more compactness of the lauroyl (C12) chain than the decanoyl (C10) and stearoyl (C18) chains.

Preprints (www.preprints.org) | NOT PEER-REVIEWED | Posted: 6 November 2023 doi:10.20944/preprints202311.0365.v1

3.6.1. Molecular orbitals (MO) analysis

Frontier molecular orbitals (FMO) in the form of HOMO (highest occupied molecular orbital) and LUMO (lowest unoccupied molecular orbital) were calculated from the DFT (B3LYP/6-31G*) optimized structures. The HOMO/LUMO energy levels, energy gap, hardness (η), and softness (S) of CFA esters **2**-**8** are mentioned in Table 8 (Figure 6). It is evident from Table 8 that the addition of ester group(s) gradually increased their HOMO-LUMO energy gap. Consequently, the sugar esters hardness value rises and softness decreases.

Table 8. Energy (eV) of HOMO, LUMO, energy gap, hardness, and softness of **2**-**8**.

Drug	*ε*HOMO	*ε*LUMO	Gap	Hardness (*η*)	Softness (*S*)
1	-7.014	-1.288	5.726	2.863	0.349
2	-7.048	-0.307	6.641	3.371	0.297
3	-7.215	-0.771	6.444	3.222	0.310
4	-7.299	-0.752	6.547	3.274	0.305
5	-7.292	-0.681	6.611	3.306	0.302
6	-6.819	-0.313	6.506	3.253	0.307
7	-6.731	-0.577	6.154	3.077	0.325
8	-7.296	-0.663	6.633	3.317	0.301

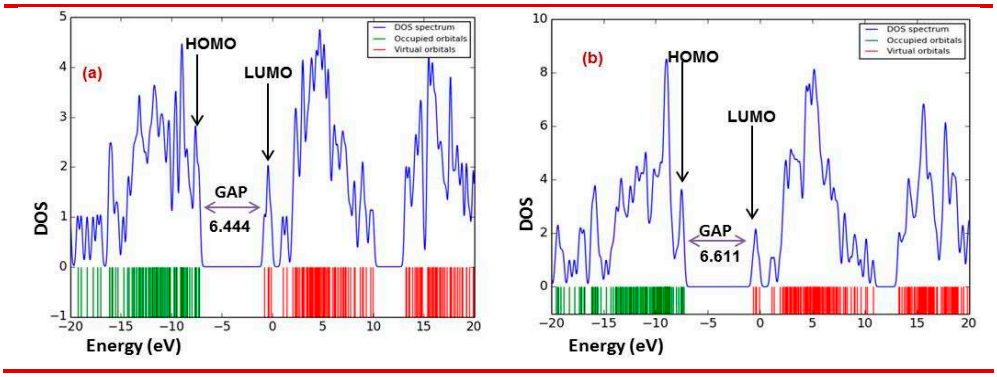

Figure 6. HOMO-LUMO energy gap and DOS plot of (*a*) **3**, and (*b*) **5**.

3.6.2. Molecular electrostatic potential (MEP) analysis

The molecular electrostatic potential (MEP) of the CFA esters was calculated and presented in Figure 7. Generally, active sites are denoted by color presentation as the red color represents the maximum negative area and is a favorable site for the electrophilic attack, the blue color indicates the maximum positive area and is a favorable site for nucleophile attack, and the green color represents zero potential areas. With the incorporation of ester groups, both the negative red and positive blue color of the CFA esters increased than the precursor MDM. However, the comparatively positive red color increased more, and hence, indicated that these MDM esters are more suitable for electrophilic reactions with the substrates, proteins, or enzymes.

Preprints (www.preprints.org) | NOT PEER-REVIEWED | Posted: 6 November 2023 doi:10.20944/preprints202311.0365.v1

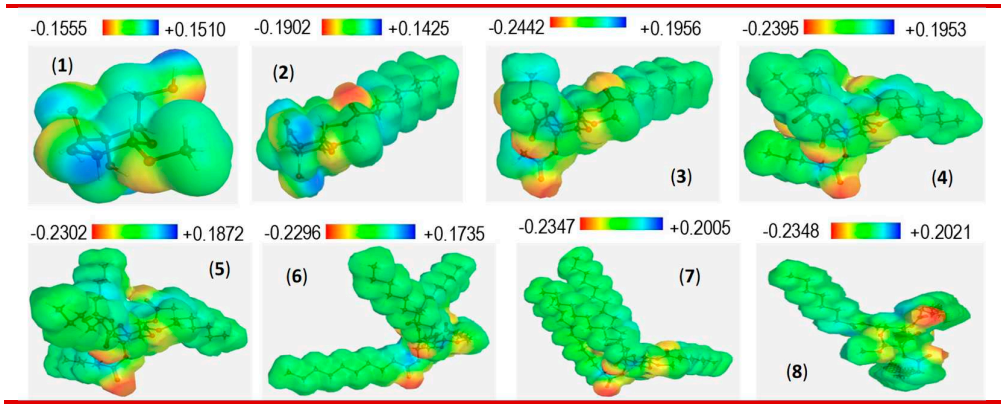

Figure 7. Molecular electrostatic potential (ev) of mannopyranosides **1**-**8**.

3.7. Drug-likeness and ADMET analysis of 2-8

Absorption, distribution, metabolism, excretion, and toxicity (ADMET) constitute the pharmacokinetic profiles of a drug molecule. Today, *in silico* ADMET studies are often used to screen for promising drug candidates and minimize the risk of failure during the drug development process rather than *in vivo* tests [53]. Herein, we used SwissADME [54,55] and admetSAR [56] for predicting the drug-likeness and ADMET properties of compounds **1**–**8** (Table 9). The results suggested that compounds **1**–**3** have good drug-likeness such as MLogP (Moriguchi octanol-water partition coefficient) values from -2.40–1.00 (<5) and topological PSA values from 99.38–123.66 (<140 Å^2), indicating that they should have good oral bioavailability. Compounds **1**-**3** also followed Lipinski drug-likeness rule (Table 9). In terms of the Lipinski rule, compounds **4**-**8** violated only higher molecular weight (MW>500). In addition, compounds **6**-**8** have moderate MLogP (>4.15). Thus, fully esterified compounds have moderate drug-likeness properties.

Table 9. Calculated HLB, drug-likeness and ADMET parameters for compounds **1**–**8**.

Compound	MW	HLB	TPSA	MLog P	Aqueous solubility	Lipinski rule		Human intestinal absorption	P-glycoprotein	Carcinogen	Acute oral toxicity	Rat acute toxicity LD_{50}	BBB
						follow	violation						
1	194.18	10.29	99.38	-2.40	Soluble	Yes	0	-0.8373	NI 0.9393	NC 0.9654	III	1.1350	N
2	320.38	8.98	105.45	-0.21	Soluble	Yes	0	-0.6797	NI 0.7283	NC 0.9671	III	2.0091	N
3	346.49	9.31	123.66	1.00	Soluble	Yes	0	0.8974	I 0.8144	NC 0.9027	III	1.9138	Y
4	572.74	7.26	123.66	2.85	Soluble	Yes	1	0.8974	I 0.8144	NC 0.9027	III	1.9138	Y
5	614.82	6.76	123.66	3.41	Poor	Yes	1	0.8974	I 0.8144	NC 0.9027	III	1.9138	Y
6	783.14	5.31	123.66	5.49	Poor	No	2	0.8974	I 0.8144	NC 0.9027	III	1.9138	Y
7	867.30	4.79	123.66	6.44	Insoluble	No	2	0.8974	I 0.8144	NC 0.9027	III	1.9138	Y
8	1119.79	3.71	123.66	9.06	Insoluble	No	2	0.8974	I 0.8144	NC 0.9027	III	1.9138	Y

MW: molecular weight; HLB: hydrophile-lipophile balance; TPSA: topological polar surface area; log P: logarithm of octanol–water partition coefficient; NI = non-inhibitor; I = inhibitor; BBB: blood–brain barrier; LD_{50} in mol/Kg.

Preprints (www.preprints.org) | NOT PEER-REVIEWED | Posted: 6 November 2023 doi:10.20944/preprints202311.0365.v1

Compounds **3**–**8** are potentially P-glycoprotein inhibitors, which can attenuate P-glycoprotein's function as a drug transporter [57]. They were expected to be non-carcinogenic but showed acute oral toxicity category-III, indicating that they should be used with caution. Compounds **3**–**8** were also expected to pass through the blood-brain barrier (BBB).

3.8. Structure-activity relationship (SAR)

As mentioned in the PASS scrutiny and *in vitro* test sections that the MDM esters were found more susceptible against several fungal pathogens than that of tested bacterial organisms. However, only a selective mannopyranoside based CFA esters exhibited considerable activity *in vitro* and comparable to the standard antifungal antibiotics (NST, FCZ, PCD). Hence, SAR was derived from combined results of the *in vitro* antimicrobial tests (Tables 4 and 5), docking scores (Table 6) and hydrophobic interactions of MDM esters with key enzyme 3LD6 (lanosterol 14α-demethylase).

Firstly, attachment of acyl group from mono to multiple and elongation of chain length (C2 to C18) gradually increased hydrophobicity of the MDM esters. Hydrophobicity, an important parameter, is related to bioactivity such as toxicity or alteration of membrane integrity and hence it is directly related to membrane permeation [31]. Hydrophobicity MDM esters gradually increased from **2** to **8**, and thus nonbonding hydrophobic interactions between acyl chains and lipid regions in the organism membrane gradually increased. Consequently, fungi/bacteria lose their membrane permeability and ultimately causing death of the organism [31].

Secondly, it was interesting to know whether CFA esters (**2-8**) or their hydrolyzed fatty acid (CA, LA, SA etc.) is responsible for the activity. The lanosterol 14α-demethylase binding affinity (Table 5) indicated lower value (CA, -4.9 kcal/mol; LA -5.0 kcal/mol; SA -4.8 kcal/mol) than MDM ester **7** (-7.7 Kcal/mol, other esters have also higher negative values -5.0 to -6.4). If hydrolysis occurred in fungal/bacterial cell wall or membrane then the resulting MDM sugar must show similar *in vitro* results, which were not found practically (in fact use of such MDM as control showed no zone of inhibition, Tables 4 and 5). These observations supported that MDM esters are responsible for the activity and were found in agreement with some reported articles [58].

Finally, we considered the effect of chain length and positional effect on antifungal activity. In most of the sugar esters in pyranoside form capryl (C8) and lauroyl (C12) chains were found more effective [22]. In the present study, one capryl and three lauroyl groups containing **7** exhibited very good *in vitro* antifungal activities along with greater binding affinity (-7.7 kcal/mol) with 3LD6. Positional changes of such group(s) also changed activity profile. For example, previously we observed that caprylic groups at C-2, C-3 and C-4 positions and lauric at C-6 position increased the antimicrobial potentiality of MDM (**1**) [29]. In our present MDM esters, positional interchange i.e. caprylic (C8) chain at C-6 position and lauric (C12) chains at C-2, C-3 and C-4 positions, as in **7**, showed better efficacy compared to previous our previous result (-5.1 kcal/mol; [29]) along with highest binding energy (-7.7 kcal/mol) which was better than nystatin (-5.6 kcal/mole) and fluconazole (-6.5 kcal/mol).

3.9. Probable antifungal mechanism of action

Ergosterol (lack of C-14 methyl group; Figure 8) is very essential for bioregulation and integrity of membrane in fungal cells. This structure is quite different from the cholesterol present (position and number of double bonds and side chains) in mammalian cells [59]. Fungal ergosterol is biosynthesized from lanosterol *via* demethylation of its C-14 methyl group. In fungi, cytochrome P450 enzyme (CYP51A1/3LD6), also known as lanosterol 14α-demethylase, catalyzes the demethylation of lanosterol to create the necessary precursor which is eventually converted into ergosterol [59]. Thus, most of the commercial antifungal drugs (fluconazole; itraconazole; voriconazole; terbinafine) are designed to deter the activity of the CYP51A1 enzyme. Due to the inactivity of CYP51A1 fungi could not synthesize ergosterol which ultimately causes disruption of the fungal cell wall [60].

As most of the antifungal drugs like triazoles have a greater affinity for fungal compared with mammalian P450 enzymes, our molecular docking score results (Table 6) and SAR studies led us to propose the following mechanism (Figure 8) for antifungal action by MDM ester **7**, which restrict

Preprints (www.preprints.org) | NOT PEER-REVIEWED | Posted: 6 November 2023 doi:10.20944/preprints202311.0365.v1

CYP51/3LD6 enzyme activity by binding with it and hence fungal lanosterol couldn't proceed for next step ultimately deter the formation of ergosterol.

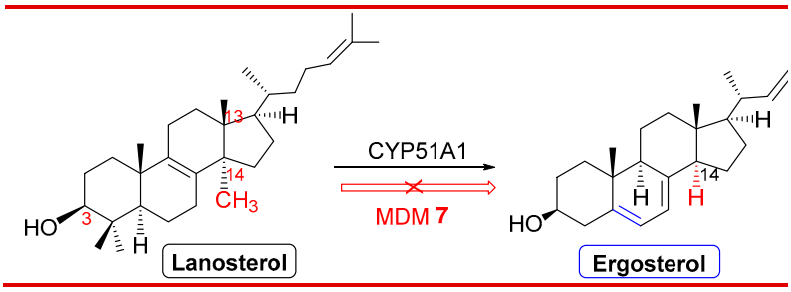

Figure 8. Probable mechanism for antifungal activity of MDM esters.

4. Conclusions

The current work presents a thorough assessment of the effects of acylation site and fatty acid chain length on the antimicrobial activity of mannopyranoside esters. Although not profoundly observed in bacteria due to inactivity, both the acylation site and the fatty acid chain length of mannopyranoside esters significantly affect their antifungal activity. Based on the structure-activity relationship (SAR) analysis, mannopyranoside esters with C12 chains were more potent against *Aspergillus* species. In terms of acylation site, mannopyranoside esters with a C8 chain substituted at the 6-*O* position were more active in the antimicrobial inhibition. Compound **7**, which fulfills these criteria, was the most potent inhibitor against *A. flavus* and *A. niger* with percentages of inhibition higher than that of fluconazole. Compound **3** with a shorter C2 chain at the 2-, 3-, and 4-*O* acylation sites seemed to be selectively active against *A. niger*. Based on the *in vitro* and docking results, compound **7** was found to interact better with lanosterol 14α-demethylase and urate oxidase than glucoamylase. Both *in vitro* experimental and *in silico* results were in agreement with these findings, suggesting that lipid-like fatty acyl group bearing these mannopyranoside oligoesters may be suitable to be developed into pharmaceutically useful materials.

Supplementary Materials: The following supporting information can be downloaded at the website of this paper posted on Preprints.org, Figures S1–S50.

Author Contributions: Conceptualization, Mohsin Kazi and Mohammed Mahbubul Matin; Methodology, Md. Lutfor Rahaman and Md. Atiqur Rahman; Software, Mohammad Amran and Talha Bin Emran; Validation, Md. Abdul Majed Patwary and Mohsin Kazi; Formal analysis, Md. Atiqur Rahman, Md. Mohin Hasnain and Mohammed Mahbubul Matin; Investigation, Md. Lutfor Rahaman, Md. Mohin Hasnain and Md Ashikur Rahaman Khan; Resources, Talha Bin Emran, Md. Abdul Majed Patwary and Mohsin Kazi; Data curation, Mohammad Amran; Writing – original draft, Mohammed Mahbubul Matin; Writing – review & editing, Md. Abdul Majed Patwary and Mohammed Mahbubul Matin; Visualization, Md Ashikur Rahaman Khan; Project administration, Mohammed Mahbubul Matin; Funding acquisition, Mohsin Kazi and Mohammed Mahbubul Matin.

Funding: The authors are grateful to the Ministry of Science and Technology, Bangladesh for partial financial support (2023-2024). The authors would like to extend their sincere appreciation to the Researchers Supporting Project Number (RSP2023R301), King Saud University, Riyad, Saudi Arabia.

Institutional Review Board Statement: Not applicable.

Informed Consent Statement: Not applicable.

Data Availability Statement: Samples and spectra of the compounds are available from the authors.

Acknowledgments: The authors would like to extend their sincere appreciation to the Researchers Supporting Project Number (RSP2023R301), King Saud University, Riyad, Saudi Arabia. M.M. is thankful to the Ministry of Science and Technology, Bangladesh for partial financial support (2023-2024).

Conflicts of Interest: The authors declare no conflict of interest. The funders had no role in the design of the study; in the collection, analyses, or interpretation of data; in the writing of the manuscript; or in the decision to publish the results.

References

1. Moutinho, L.F.; Moura, F.R.; Silvestre, R.C.; Romao-Dumaresq, A.S. Microbial biosurfactants: A broad analysis of properties, applications, biosynthesis, and techno-economical assessment of rhamnolipid production. *Biotechnol. Prog.* **2021**, *37*(2), e3093. https://doi.org/10.1002/btpr.3093
2. Gumel, A.M.; Annuar, M.S.M.; Heidelberg, T.; Chisti, Y. Lipase mediated synthesis of sugar fatty acid esters. *Process. Biochem.* **2011**, *46*, 2079-2090. https://doi.org/10.1016/j.procbio.2011.07.021
3. Plat, T.; Linhardt, R.J. Syntheses and applications of sucrose-based esters. *J. Surfact. Deter.* **2001**, *4*, 415-421. https://doi.org/10.1007/s11743-001-0196-y
4. Nobmann, P.; Bourke, P.; Dunne, J.; Henehan, G. In vitro antimicrobial activity and mechanism of action of novel carbohydrate fatty acid derivatives against Staphylococcus aureus and MRSA. *J. Appl. Microbiol.* **2010**, *108*, 2152-2161. https://doi.org/10.1111/j.1365-2672.2009.04622.x
5. Zhao, L.; Zhang, H.Y.; Hao, T.Y.; Li, S.R. In vitro antibacterial activities and mechanism of sugar fatty acid esters against five food-related bacteria. *Food Chem*. **2015**, *187*, 370-377. https://doi.org/10.1016/j.foodchem.2015.04.108
6. Lucarini, S.; Fagioli, L.; Campana, R.; Cole, H.; Duranti, A.; Baffone, W.; et al. Unsaturated fatty acids lactose esters: cytotoxicity, permeability enhancement and antimicrobial activity. *Eur. J. Pharm. Biopharm*. **2016**, *107*, 88-96. https://doi.org/10.1016/j.ejpb.2016.06.022
7. Shao, S.-Y.; Shi, Y.-G.; Wu, Y.; Bian, L.-Q.; Zhu, Y.-J.; Huang, X.-Y.; et al. Lipase-catalyzed synthesis of sucrose monolaurate and its antibacterial property and mode of action against four pathogenic bacteria. *Molecules* **2018**, *23*, e1118. https://doi.org/10.3390/molecules23051118
8. Staron, J.; Dabrowski, J.M.; Cichon, E.; Guzik. M. Lactose esters: synthesis and biotechnological applications. *Critic. Rev. Biotech.* **2018**, *38*, 245-258. https://doi.org/10.1080/07388551.2017.1332571
9. Huang, X.B.; Zhang, B.C.; Xu, H. Synthesis of some monosaccharide-related ester derivatives as insecticidal and acaricidal agents. *Bioorg. Med. Chem. Lett.* **2017**, *27*, 4336-4340. https://doi.org/10.1016/j.bmcl.2017.08.031
10. Okamoto, H.; Sakai, T.; Danjo, K. Effect of sucrose fatty acid esters on transdermal permeation of lidocaine and ketoprofen. *Biol. Pharmaceutic. Bull.* **2005**, *28*, 1689-1694. https://doi.org/10.1248/bpb.28.1689
11. Ei-Laithy, H.M.; Shoukry, O.; Mahran,. L.G. Novel sugar esters proniosomes for transdermal delivery of vinpocetine: Preclinical and clinical studies. *Eur. J. Pharm. Biopharm.* **2011**, *77*, 43-55. https://doi.org/10.1016/j.ejpb.2010.10.011
12. Okamoto, H.; Sakai, T.; Tokuyama, C.; Danjo, K. Sugar ester J-1216 enhances percutaneous permeation of ionized lidocaine. *J. Pharm. Sci.* **2011**, *100*, 4482-4490. https://doi.org/10.1002/jps.22644
13. Alama, T.; Katayama, H.; Hirai, S.; Ono, S.; Kajiyama, A.; Kusamori, K. et al. Enhanced oral delivery of alendronate by sucrose fatty acids esters in rats and their absorption-enhancing mechanisms. *Int. J. Pharm.* **2016**, *515*, 476-489. https://doi.org/10.1016/j.ijpharm.2016.10.046
14. Perinelli, D.R.; Lucarini, S.; Fagioli, L.; Campana, R.; Vllasaliu, D.; Duranti, A. et al. Lactose oleate as new biocompatible surfactant for pharmaceutical applications. *Eur. J. Pharm. Biopharm.* **2018**, *124*, 55-62. https://doi.org/10.1016/j.ejpb.2017.12.008
15. Teng, Y.L.; Stewart, S.G.; Hai, Y.W.; Li, X.; Banwell, M.G.; Lan, P. Sucrose fatty acid esters: Synthesis, emulsifying capacities, biological activities and structure-property profiles. *Critic. Rev. Food Sci. Nutr.* **2021**, *61*, 3297-3317. https://doi.org/10.1080/10408398.2020.1798346
16. Sanaullah, A.F.M.; Bhuiyan, M.M.H.; Matin, M.M. Stearoyl glucopyranosides: Selective synthesis, PASS analysis, in vitro antimicrobial, and SAR study. *Egyp. J. Chem.* **2022**, *65*(9), 329-338. https://doi.org/10.21608/ejchem.2022.111831.5080
17. AlFindee, M.N.; Zhang, Q.; Subedi, Y.P.; Shrestha, J.P.; Kawasaki, Y.; Grilley, M. et al. (2018). One-step synthesis of carbohydrate esters as antibacterial and antifungal agents. *Bioorg. Med. Chem.* 26, 765-774. https://doi.org/10.1016/j.bmc.2017.12.038
18. Watanabe, T.; Katayama, S.; Matsubara, M.; Honda, Y.; Kuwahara, M. Antibacterial carbohydrate monoesters suppressing cell growth of Streptococcus mutans in the presence of sucrose. *Curr. Microbiol.* **2000**, *41*, 210-213. https://doi.org/10.1007/s002840010121
19. Snoch, W.; Stepien, K.; Prajsnar, J.; Staron, J.; Szaleniec, M.; Guzik, M. Influence of chemical modifications of polyhydroxyalkanoate-derived fatty acids on their antimicrobial properties. *Catalysts* **2019**, *9*, e510. https://doi.org/10.3390/catal9060510
20. Petkova, N.; Vassilev, D.; Grudeva, R.; Tumbarski, Y.; Vasileva, I. et al. "Green" Synthesis of sucrose octaacetate and characterization of its physicochemical properties and antimicrobial activity. *Chem. Biochem. Engin. Quart.* **2017**, *31*, 395-402. https://doi.org/10.15255/CABEQ.2017.1117
21. Matin, M.M.; Nath, A.R.; Saad, O.; Bhuiyan, M.M.H.; Kadir, F.A.; Hamid, S.B.A. et al. Synthesis, PASS-predication and in vitro antimicrobial activity of benzyl 4-*O*-benzoyl-α-L-rhamnopyranoside derivatives. *Int. J. Mol. Sci.* **2016**, *17*, e1412. https://doi.org/10.3390/ijms17091412
22. Matin, M.M.; Bhattacharjee, S.C.; Chakraborty, P.; Alam, M.S. Synthesis, PASS predication, in vitro antimicrobial evaluation and pharmacokinetic study of novel n-octyl glucopyranoside esters. *Carbohydr. Res.* **2019**, *485*, e107812. https://doi.org/10.1016/j.carres.2019.107812

23. Stegemann, S.; Leveiller, F.; Franchi, D.; de Jong, H.; Linden, H. When poor solubility becomes an issue: From early stage to proof of concept. *Eur. J. Pharm. Sci.* **2007**, *31*, 249-261. https://doi.org/10.1016/j.ejps.2007.05.110
24. Aronson, M.; Medalia, O.; Schori, L.; Mirelman, D.; Sharon, N.; Ofek. I. (1979). Prevention of colonization of the urinary tract of mice with Escherichia coli by blocking of bacterial adherence with methyl alpha-D-mannopyranoside. *J. Infect. Dis.* **1979**, *139*, 329-332. doi: 10.1093/infdis/139.3.329
25. Matsumura, S.; Imai, K.; Yoshikawa, S.; Kawada, K.; Uchibor, T. Surface activities, biodegradability and antimicrobial properties of n-alkyl glucosides, mannosides and galactosides. *J. Am. Oil Chem. Soc.* **1990**, *67*, 996-1001. https://doi.org/10.1007/BF02541865
26. Okamoto, H.; Sakai, T.; Tokuyama, C.; Danjo, K. Sugar ester J-1216 enhances percutaneous permeation of ionized lidocaine. *J. Pharm. Sci.* **2011**, *100*, 4482-4490. https://doi.org/10.1002/jps.22644
27. Zhang, Y.H.; Chen, L.Q.; Wu, X.B. Thermotropic liquid crystalline and surface-active properties of n-alkyl alpha-D-mannopyranosides. *J. Mol. Liq.* **2018**, *269*, 947-955. https://doi.org/10.1016/j.molliq.2018.02.017
28. Hanee, U.; Rahman, M.R.; Matin, M.M. Synthesis, PASS, in silico ADMET, and thermodynamic studies of some galactopyranoside esters. *Phys. Chem. Res.* **2021**, *9*(4), 591-603. https://doi.org/10.22036/pcr.2021.282956.1911
29. Matin, M.M.; Bhuiyan, M.M.H.; Kabir, E.; Sanaullah, A.F.M.; Rahman, M.A.; Hossain, M.E. et al. Synthesis, characterization, ADMET, PASS predication, and antimicrobial study of 6-*O*-lauroyl mannopyranosides. *J. Mol. Struct.* **2019**, *1195*, 189-197. https://doi.org/10.1016/j.molstruc.2019.05.102
30. Matin, M.M.; Uzzaman, M.; Chowdhury, S.A.; Bhuiyan, M.M.H. In vitro antimicrobial, physicochemical, pharmacokinetics and molecular docking studies of benzoyl uridine esters against SARS-CoV-2 main protease. *J. Biomol. Struct. Dyn.* **2022**, *40*(8), 3668-3680. https://doi.org/10.1080/07391102.2020.1850358
31. Matin, M.M.; Chakraborty, P.; Alam, M.S.; Islam, M.M.; Hanee,. U. Novel mannopyranoside esters as sterol 14 alpha-demethylase inhibitors: Synthesis, PASS predication, molecular docking, and pharmacokinetic studies. *Carbohydr. Res.* **2020**, *496*, e108130. https://doi.org/10.1016/j.carres.2020.108130
32. Park, K.M.; Lee, S.J.; Yu, H. et al. Hydrophilic and lipophilic characteristics of non-fatty acid moieties: significant factors affecting antibacterial activity of lauric acid esters. *Food Sci. Biotechnol.* **2018**, *27*, 401-409. doi: 10.1007/s10068-018-0353-x
33. Wagh, A.; Shen, S.; Shen, F.A.; Miller, C.D.; Walsh, M.K. Effect of lactose monolaurate on pathogenic and nonpathogenic bacteria. *Appl. Environ. Microbiol.* **2012**, *78*(9), 3465-3468. https://doi.org/10.1128/AEM.07701-11
34. Nakayama, M.; Tomiyama, D.; Ikeda, K.; Katsuki, M.; Nonaka, A.; Miyamoto, T. Antibacterial effects of monoglycerol fatty acid esters and sucrose fatty acid esters on bacillus spp. *Food Sci. Technol. Res.* **2015**, *21*, 431-437. https://doi.org/10.3136/fstr.21.431
35. Zhang, X.; Song, F.; Taxipalati, M.; Wei, W.; Feng, F. Comparative study of surface-active properties and antimicrobial activities of disaccharide monoesters. *Plos One* **2014**, *9*, e114845. https://doi.org/10.1371/journal.pone.0114845
36. Zhang, X.; Wei, W.; Cao, X.; Feng, F. Characterization of enzymatically prepared sugar medium-chain fatty acid monoesters. *J. Sci. Food Agric.* **2015**, *9*, 1631-1637. https://doi.org/10.1002/jsfa.6863
37. Matin, M.M.; Hasan, M.S.; Uzzaman, M.; Bhuiyan, M.M.H.; Kibria, S.M.; Hossain, M.E.; Roshid, M.H.O. Synthesis, spectroscopic characterization, molecular docking, and ADMET studies of mannopyranoside esters as antimicrobial agents. *J. Mol. Struct.* **2020**, *1222*, 128821. https://doi.org/10.1016/j.molstruc.2020.128821
38. Clinical and Laboratory Standards Institute. Methods for antimicrobial susceptibility testing of anaerobic bacteria: approved standard-8th ed. CLSI document, Approved Standard M11-A8. Wayne, PA: Clinical and Laboratory Standards Institute; **2012**.
39. Grover, R.K.; Moore, J.D. Toximetric studies of fungicides against the brown rot organisms Sclerotinia fluticola and S. laxa. *Phytopathol*. **1962**, *52*, 876-880.
40. Akash, S.; Kumer, A.; Chandro, A.; Chakma, U.; Matin, M.M. Quantum calculation, docking, ADMET and molecular dynamics of ketal and non-ketal forms of D-glucofuranose against bacteria, black & white fungus, and triple-negative breast cancer. *Bioint. Res. Appl. Chem*. **2023**, *13*(4), 374. https://doi.org/10.33263/BRIAC134.374
41. Kumer, A.; Chakma, U.; Chandro, A.; Howlader, D.; Akash, S.; Kobir, M.E.; Hossain, T.; Matin, M.M. Modified D-glucofuranose computationally screening for inhibitor of breast cancer and triple breast cancer: Chemical descriptor, molecular docking, molecular dynamics and QSAR. *J. Chilean Chem. Soc*. **2022**, *67*(3), 5623-5635. http://dx.doi.org/10.4067/S0717-97072022000305623
42. Kumer, A.; Chakma, U.; Matin, M.M. Bilastine based drugs as SARS-CoV-2 protease inhibitors: Molecular docking, dynamics, and ADMET related studies. *Orbital: Electron. J. Chem.* **2022**, *14*(1), 15-23. http://dx.doi.org/10.17807/orbital.v14i1.1642

43. Matin, M.M.; Ibrahim, M.; Anisa, T.R.; Rahman, M.R. Synthesis, characterization, in silico optimization, and conformational studies of methyl 4-O-palmitoyl-α-L-rhamnopyranosides. *Malaysian J. Sci.* **2022**, *41*(1), 91-105. https://doi.org/10.22452/mjs.vol41no1.6
44. Griffin, W.C. Calculation of HLB values of non-ionic surfactants. *J. Soc. Cos. Chem.* **1954**, *5*, 249-256.
45. Syed, S.B.; Arya, H.; Fu, I.-H.; Yeh, T.-K.; Periyasamy, L.; Hsieh, H.-P.; Coumar, M.S. Targeting P-glycoprotein: Investigation of piperine analogs for overcoming drug resistance in cancer. *Sci. Rep.* **2017**, *7*, 7972. https://doi.org/10.1038/s41598-017-08062-2
46. Daina, A.; Michielin, O.; Zoete, V. SwissADME: a free web tool to evaluate pharmacokinetics, drug-likeness and medicinal chemistry friendliness of small molecules, *Sci. Rep.* **2017**, *7*, 42717. https://doi.org/10.1038/srep42717
47. Matin, M.M.; Bhuiyan, M.M.H.; Kibria, S.M.; Hasan, M.S. Synthesis, PASS predication of antimicrobial activity and pharmacokinetic properties of hexanoyl galactopyranosides and experimental evaluation of their action against four human pathogenic bacteria and four fungal strains. *Pharm. Chem. J.* **2022**, *56*(5), 627-637. https://doi.org/10.1007/s11094-022-02687-y
48. Matin, P.; Hanee, U.; Alam, M.S.; Jeong, J.E.; Matin, M.M.; Rahman, M.R.; Mahmud, S.; Alshahrani, M.M.; Kim, B. Novel galactopyranoside esters: Synthesis, mechanism, in vitro antimicrobial evaluation and molecular docking studies. *Molecules* **2022**, *27*(13), 4125. https://doi.org/10.3390/molecules27134125
49. AFM Sanaullah, MM Matin, MR Rahman, SMA Nayeem, Acyl glucopyranosides: Synthesis, PASS predication, antifungal activities, and molecular docking. *Org. Communications* **2022**, 15(1), 32-43. http://doi.org/10.25135/acg.oc.120.2201.2307
50. Ahuja, R.; Sidhu, A.; Bala, A.; Arora, D.; Sharma, P. Structure based approach for twin-enzyme targeted benzimidazolyl-1,2,4-triazole molecular hybrids as antifungal agents. *Arabian J. Chem.* **2020**, *13*, 5832–5848. https://doi.org/10.1016/j.arabjc.2020.04.020
51. Chugunova, E.; Shaekhov, T.; Khamatgalimov, A.; Gorshkov, V.; Burilov, A. DFT Quantum-Chemical Calculation of Thermodynamic Parameters and DSC Measurement of Thermostability of Novel Benzofuroxan Derivatives Containing Triazidoisobutyl Fragments. *Int. J. Mol. Sci.* **2022**, *23*(3), 1471. https://doi.org/10.3390/ijms23031471.
52. Rahman, M.A.; Matin, M.M.; Kumer, A.; Chakma, U.; Rahman, M.R. Modified D-glucofuranoses as new black fungus protease inhibitors: Computational screening, docking, dynamics, and QSAR study. *Phy. Chem. Res.* **2022**, *10*(2), 195-209. https://doi.org/10.22036/pcr.2021.294078.1934
53. Munawar, A.; Zaman, F.; Ishaq, M.W.; Hassan, K.A.; Masood, S.; Ali, Z.; et al. Comparative study to characterise the pharmaceutical potential of synthesised snake venom Bradykinin-Potentiating peptides in vivo. *Curr. Med. Chem*. **2022**, *29*, 6422-6432. https://doi.org/10.2174/0929867329666220203153051
54. Muhammad, D.; Matin, M.M.; Miah, S.M.R.; Devi, P. Synthesis, antimicrobial, and DFT studies of some benzyl 4-O-acyl-α-L-rhamnopyranosides. *Orbital: Electron. J. Chem.* **2021**, *13*(3), 250-258. https://doi.org/10.17807/orbital.v13i3.1614
55. Sanaullah, A.F.M.; Devi, P.; Hossain, T.; Sultan, S.B.; Badhon, M.M.U.; Hossain, M.E.; Uddin, J.; Patwary, M.A.M.; Kazi, M.; Matin, M.M. Rhamnopyranoside-based fatty acid esters as antimicrobials: Synthesis, spectral characterization, PASS, antimicrobial, and molecular docking studies. *Molecules* **2023**, *28*, 986. https://doi.org/10.3390/molecules28030986
56. Cheng, F.X.; Li, W.H.; Zhou, Y.D.; Shen, J.; Wu, Z.R.; Liu, G.X. et al. admetSAR: A comprehensive source and free tool for assessment of chemical ADMET properties. *J. Chem. Inform. Model.* **2012**, *52*, 3099-3105. https://doi.org/10.1021/ci300367a
57. Aller, S.G.; Yu, J.; Ward, A.; Weng, Y.; Chittaboina, S.; Zhuo, R.P. et al. Structure of P-glycoprotein reveals a molecular basis for poly-specific drug binding. *Science* **2009**, *323*, 1718-22. https://doi.org/10.1126/science.1168750
58. Nobmann, P.; Smith, A.; Dunne, J.; Henehan, G.; Bourke, P. The antimicrobial efficacy and structure activity relationship of novel carbohydrate fatty acid derivatives against *Listeria spp.* and food spoilage microorganisms. *Int. J. Food Microb.* **2009**, *128*, 440-445.
59. Lepesheva, G.I.; Waterman, M.R. Sterol 14α-demethylase cytochrome P450 (CYP51), a P450 in all biological kingdoms. *Biochim. Biophys. Acta*. **2007**, *1770*(3), 467-477. https://doi.org/10.1016/j.bbagen.2006.07.018
60. Ghannoum, M.A.; Rice, L.B. Antifungal agents: Mode of action, mechanisms of resistance, and correlation of these mechanisms with bacterial resistance. *Clin. Microbiol. Rev.* **1999**, *12*(4), 501-517. https://doi.org/10.1128/CMR.12.4.501